On thermo-acoustic acoustic-vortical-entropy waves and flow stability

L. M. B. C. Campos* A. C. Marta

Center for Aeronautical and Space Science and Technology
IDMEC/LAETA, Instituto Superior Técnico, Universidade de Lisboa
Av. Rovisco Pais 1, 1049-001 Lisboa, Portugal

5th CEAS Air & Space Conference

Abstract

The noise of jet and rocket engines involves the coupling of sound to swirling flows and to heat exchanges leading in the more complex cases of triple interactions to acoustic-vortical-entropy (AVE) waves. The present paper presents as far as the authors are aware the first derivation of the AVE equation for axisymmetric linear non-dissipative perturbations of a compressible, non-isentropic, swirling mean flow, with constant axial velocity and constant angular velocity. The axisymmetric AVE wave equation is obtained for the radial velocity perturbation, specifying its radial dependence for a given frequency and axial wavenumber. The AVE wave equation in the case of zero axial wavenumber has only one singularity at the critical radius, where the isothermal Mach number for the swirl velocity is unity. The exact solution of the AVE wave equation is obtained as series expansions of Gaussian hypergeometric type valid inside, outside and around the critical layer, thus: (i) covering the whole flow region; (ii) identifying the singularity at the sonic condition at the critical layer; (iii) specifying near-axis and asymptotic solutions for small and large radius. Using polarization relations among wave variables specifies exactly the perturbations of: (i,ii) the radial and azimuthal velocity; (iii,iv) pressure and mass density; (v,vi) entropy and temperature. It is shown that the dependence of the AVE wave variables on the radial distance can be: (a) oscillatory with decaying amplitude; (b) monotonic with increasing amplitude. The case (b) of AVE wave amplitude increasing monotonically with the radial distance applies if the frequency times a function of the adiabatic exponent is less than the vorticity (or twice the angular velocity). In the opposite case (a) the oscillatory nature of acoustic waves predominates over the tendency for monotonic growth of vortical perturbations. Associating sound with stable potential flows and swirl with unstable vortical flows suggests a criterion valid in non-isentropic conditions, that is in the presence of heat exchanges, that is a condition for stable combustion in a confined space: the peak vorticity (multiplied by a factor of order unity dependent on the adiabatic exponent) should be less than the lowest or fundamental frequency of the cavity.

1 Introduction

The noise of aircraft engines is a major limitation on airport operations, and the subject of ever more stringent certification rules, aiming to limit the total noise exposure as air traffic grows. The noise of the rocket engines of space launchers are sufficiently high to cause structural damage and require payloads like satellites to be tested in reverberant chambers. The literature on aircraft and rocket noise usually considers purely acoustic waves, although coupling with other modes occur in: (i) inlet ducts due to the shear flow in the wall boundary layers; (ii) in turbine exhausts due to the downstream swirling flow; (iii) in the combustion chambers and other heat generation and exchange

*Corresponding author: luis.campos@tecnico.ulisboa.pt

processes involving non-isentropic flows. In spite of the practical ubiquity of these phenomena, the present paper may be one of the first to consider the triple interaction of acoustic, vortical and entropy perturbations.

There are (1; 2; 3) three types of waves in a fluid in the absence of external restoring forces (4; 5), namely: (i) sound waves that are longitudinal and compressive; (ii) vortical waves that are transversal, hence incompressible; (iii) entropy modes associated with heat exchanges, hence non-isentropic flow. The acoustic modes receive most attention because for an homogeneous uniform mean flow: (i) the acoustic modes satisfy the convected wave equation for uniform motion and the classical wave equation in a medium at rest (6; 7; 8; 9; 10; 11; 12); (ii) by Kelvin circulation theorem the circulation along a loop convected with the mean flow is constant (13; 14; 15; 16; 17); (iii) in homentropic conditions there are no entropy modes. The most general conditions for the existence of purely acoustic modes, decoupled from vortical-entropy modes, is a potential homentropic mean flow, that may be compressible, and leads to the high-speed wave equation (18; 19; 20) that reduces to the convected wave equation (21; 22; 23) in two cases: (i) uniform flow; (ii) low Mach number non-uniform flow. The presence of vorticity leads to acoustic-vortical-waves (24; 25; 26; 27; 28; 29), in a compressible sheared (30; 31; 32; 33; 34; 35; 36; 37; 38; 39; 40; 41; 42; 43) or swirling (44; 45; 46; 47; 48; 49; 50; 51) mean flow. The present paper considers a further extension to acoustic-vortical-entropy waves that specify the stability of a compressible, vortical non-isentropic mean flow. This includes, as far as the authors are aware, the first derivation of an acoustic-vortical-entropy (AVE) wave equation, as well as an exact solution.

The present paper: (i) is not about the generation of sound by small patches of vorticity (52; 53) or inhomogeneities (19; 20) convected in a potential flow, that is respectively 'vortex' and 'entropy' noise; (ii) it is about linear perturbations of a compressible, vortical, non-isentropic mean flow occupying all space, that may be designated acoustic-vortical-entropy waves. These perturbations determine the stability of the mean flow (54; 55; 56; 57; 58) in this case the stability of a compressible, vortical, non-isentropic flow. The paper considers what possibly is the simplest case of acoustic-vortical-entropy (AVE) waves: (i) linear non-dissipative perturbations of an axisymmetric mean flow with uniform axial velocity and rigid-body swirl; (ii) the mean flow is compressible, vortical and non-isentropic allowing for the existence of AVE waves; (iii) the perturbations depend on time, axial and radial coordinates, but not on azimuthal angle; (iv) this allows for the fundamental axisymmetric mode, but excludes all non-axisymmetric azimuthal modes. The derivation of the acoustic-vortical-entropy wave equation (Section 2): (i) is based on the linearization of the equations of continuity, inviscid momentum and energy (Subsection 2.2), using the entropy and equation of state of a perfect gas (Subsection 2.1); (ii) the elimination for the radial velocity perturbation leads to the AVE wave equation, and the remaining wave variables, namely the pressure, mass density, entropy, temperature and azimuthal velocity are expressed in terms of its solution (Subsection 2.3).

The presence of swirl leads to a radial pressure gradient in the mean flow due to the centrifugal force, and thus the sound speed varies radially; since the mean flow is assumed to be non-isentropic there is an entropy parameter, in addition to the sound speed. The acoustic-vortical-entropy wave equation specifying the radial dependence of the radial velocity perturbation spectrum for a given frequency and axial wavenumber has a singularity at a critical radius (Section 3) where the swirl velocity of the mean flow equals the isothermal sound speed, i.e. the 'sonic condition' of isothermal swirl Mach number unity (Subsection 3.1). Thus there are two solutions: (i) an inner solution in ascending power series of the radius (Subsection 3.2); (ii) an outer solution in descending power series of the radius (Subsection 3.3). The AVE wave equation can be transformed to a Gaussian hypergeometric differential equation (Section 4) thus confirming the inner (Subsection 4.1) and outer (Subsection 4.2) solution as respectively ascending and descending power series of the radius, valid respectively inside and outside the critical radius. The inner and outer solutions are matched by using a third solution valid around the critical layer that overlaps with both; this third solution is valid over the whole space and shows that the wave field is finite at the critical layer (Subsection 4.3). The solutions of the AVE wave equation are illustrated by the computation of the wave variables (Section 5). Thus the divergence of the inner and outer solutions at the critical layer is due to the failure of the power series to converge at their boundary of convergence (Subsection 5.1) and not to the wave field that is finite at the critical layer. The inner and outer solutions may be used to describe the wave in a cylinder or cylindrical annulus, respectively inside and outside

the critical layer; the solutions around the critical layer still apply also when the critical layer lies inside the cylindrical or annular duct (Subsection 5.2). The solutions of the AVE wave equation (Figures 1 and 2 and Table 1) are applied to a cylinder with rigid walls containing the critical radius (Subsection 5.3) to determine: (i) the eigenvalues for the radial wavenumber and frequency (Tables 2 and 3); (ii) the corresponding eigenfunctions or waveforms for the perturbations of the radial and azimuthal velocity, mass density, entropy, pressure and temperature as function of the radius (Figures 4 to 9). The discussion (Section 7) concerns the wave fields (Section 5) that are solutions (Section 4) of the acoustic-vortical-entropy wave equation (Section 2) and their possible relation with the stability of the compressible, vortical, non-isentropic mean flow (Section 3).

2 The acoustic-vortical-entropy wave equation

The acoustic-vortical-entropy waves are considered as small axisymmetric perturbations of an axisymmetric compressible non-isentropic mean flow (Subsection 2.1) with uniform axial velocity and rigid body swirl (Subsection 2.2). Elimination for the radial velocity perturbation leads to the acoustic-vortical-entropy wave equation, whose solutions specifies also the perturbations of azimuthal velocity, pressure, mass density, temperature and entropy (Subsection 2.3).

2.1 Compressible, vortical, non-isentropic flow of a perfect gas

The fundamental equations of fluid mechanics are written in cylindrical coordinates (r, φ, z) in axisymmetric form without φ-dependence ($\partial/\partial\varphi = 0$):
(i) mass conservation:

$$\mathrm{D}\Gamma/\mathrm{d}t = -\Gamma \boldsymbol{\nabla}\cdot\boldsymbol{V} = -\frac{\Gamma}{r}\frac{\partial}{\partial r}(rV_r) - \Gamma\frac{\partial V_z}{\partial z}\,; \tag{1}$$

(ii) inviscid momentum:

$$\Gamma\left(\mathrm{D}V_r/\mathrm{d}t - r^{-1}V_\varphi^2\right) + \partial_r P = 0\,, \tag{2a}$$

$$\Gamma\left(\mathrm{D}V_\varphi/\mathrm{d}t + r^{-1}V_r V_\varphi\right) + r^{-1}\partial_\varphi P = 0\,, \tag{2b}$$

$$\Gamma \mathrm{D}V_z/\mathrm{d}t + \partial_z P = 0\,; \tag{2c}$$

(iii) energy:

$$\Gamma T\,\mathrm{D}S/\mathrm{d}t = 0\,; \tag{3}$$

(iii) state:

$$\mathrm{D}P/\mathrm{d}t = c^2\mathrm{D}\Gamma/\mathrm{d}t + \beta\mathrm{D}S/\mathrm{d}t\,; \tag{4}$$

where Γ is the mass density, P the pressure, $\boldsymbol{V}$ the velocity, T the temperature, S the entropy, the material derivative is denoted by

$$\mathrm{D}/\mathrm{d}t = \partial/\partial t + \boldsymbol{V}\cdot\boldsymbol{\nabla} = \partial/\partial t + V_r\partial_r + V_z\partial_z\,, \tag{5a, b}$$

and the equation of state in the form (6a) specifies the coefficients in (4),

$$P = P(\Gamma, S)\,:\quad c^2 \equiv \left(\frac{\partial P}{\partial \Gamma}\right)_S\,,\quad \beta = \left(\frac{\partial P}{\partial S}\right)_\Gamma\,, \tag{6a - c}$$

namely the adiabatic sound speed (6b) and the non-isentropic coefficient (6c). Chemical reactions are not considered explicitly and appear through the entropy coefficient.

In the case of a perfect gas, the equations of state (7a) and entropy (7b),

$$P = R\Gamma T\,,\quad S = C_V\log P - C_P\log\Gamma\,, \tag{7a, b}$$

involve the gas constant R and specific heats at constant volume C_V and pressure C_P that are related by (8a,c,d) involving the adiabatic exponent (8b),

$$R = C_P - C_V\,,\quad \gamma = \frac{C_P}{C_V}\,:\quad C_V = \frac{R}{\gamma - 1}\,,\quad C_P = \frac{\gamma R}{\gamma - 1}\,. \tag{8a - d}$$

From the entropy equation (7b) it follows

$$\mathrm{d}S = C_V \frac{\mathrm{d}P}{P} - C_P \frac{\mathrm{d}\Gamma}{\Gamma}\,, \tag{9a}$$

that the adiabatic sound speed (9b) is given by (9c),

$$\mathrm{d}S = 0 \,:\quad c^2 = \left(\frac{\partial P}{\partial \Gamma}\right)_S = \frac{C_P}{C_V}\frac{P}{\Gamma} = \gamma \frac{P}{\Gamma} = \gamma R T\,. \tag{9b, c}$$

The non-isentropic coefficient (6c) may be calculated (10b) from the specific heat at constant volume (10a),

$$C_V = T\left(\frac{\partial S}{\partial T}\right)_\Gamma \,:\quad \beta = \left(\frac{\partial P}{\partial T}\right)_\Gamma \Big/ \left(\frac{\partial S}{\partial T}\right)_\Gamma = \frac{T}{C_V}\left(\frac{\partial P}{\partial T}\right)_\Gamma\,; \tag{10a, b}$$

in the case of a perfect gas (7a) follows (11a,b),

$$\beta = \frac{T}{C_V} R\Gamma = \frac{P}{C_V} = \frac{\gamma - 1}{R} P\,, \tag{11a - c}$$

and also (11c) using (8c).

2.2 Linear perturbation of a uniform flow with rigid body swirl

The mean flow is assumed to consist (12a) of a uniform axial velocity plus a rigid body swirl,

$$\boldsymbol{V}_0 = \boldsymbol{e}_z U + \boldsymbol{e}_\varphi \Omega r\,, \quad \boldsymbol{\varpi} = \boldsymbol{\nabla} \times \boldsymbol{V}_0 = \boldsymbol{e}_z 2\Omega\,, \tag{12a, b}$$

so that the vorticity (12b) is twice the angular velocity. The linearised material derivative (5a) for the mean flow (12a) is

$$\mathrm{d}/\mathrm{d}t \equiv \partial/\partial t + \boldsymbol{V}_0 \cdot \boldsymbol{\nabla} = \partial/\partial t + U \partial/\partial z\,. \tag{13}$$

Applying the fundamental equations to the mean flow (12a) it follows that: (i-ii) the mass density (1) and entropy (3) can depend only on the radius (14a,b); (iii) there is a radial pressure gradient (2a) due to the centrifugal force (14c),

$$\rho_0 = \rho_0(r)\,,\, s_0 = s_0(r) \,:\quad p_0' \equiv \mathrm{d}p_0/\mathrm{d}r = \rho_0 \Omega^2 r\,; \tag{14a - c}$$

assuming a constant mass density (15a) leads to the pressure (15c) where (15b) is the pressure on axis,

$$\rho_0 = \mathrm{const}\,,\, p_{00} = p_0(0) \,:\quad p_0(r) = p_{00} + \frac{1}{2}\rho_0 \Omega^2 r^2\,. \tag{15a - c}$$

The sound speed (9c) and non-isentropic coefficient (11b) are given in the mean flow respectively by (16b) and (16c), where (9a) is the sound speed on the axis,

$$c_{00}^2 = \gamma \frac{p_{00}}{\rho_0} \,:\quad [c_0(r)]^2 = \gamma \frac{p_0(r)}{\rho_0} = c_{00}^2 + \frac{\gamma}{2}\Omega^2 r^2\,, \quad \beta_0(r) = \frac{p_0(r)}{C_V}\,. \tag{16a - c}$$

The entropy in the mean flow (17a),

$$s_0 = C_V \log p_0 - C_P \log \rho_0\,, \tag{17a}$$

has radial gradient (17b),

$$s_0' = C_V \frac{p_0'}{p_0} = \frac{p_0'}{\beta_0} = \frac{\rho_0 \Omega^2 r}{\beta_0} = C_V \frac{\rho_0 \Omega^2 r}{p_0} = C_V \gamma \frac{\Omega^2 r}{c_0^2} = C_P \frac{\Omega^2 r}{c_0^2}\,. \tag{17b}$$

Thus the uniform axial flow with rigid body swirl (12a) and a constant mass density (15a) implies the radial dependences of the pressure (15b,c), sound speed (16a,b) and also the existence of an entropy gradient (17b). The linear perturbation of this mean flow is considered next.

The total flow is assumed to consist of the mean flow plus a perturbation depending on time t, radial r and axial z coordinate, but not on the azimuthal coordinate φ,

$$V_r(r,z,t) = v_r(r,z,t)\,, \quad V_\varphi(r,z,t) = \Omega r + v_\varphi(r,z,t)\,, \quad V_z(r,z,t) = U + v_z(r,z,t)\,, \quad (18\mathrm{a-c})$$

$$P(r,z,t) = p_0(r) + p(r,z,t)\,, \quad \Gamma(r,z,t) = \rho_0 + \rho(r,z,t)\,, \quad S(r,z,t) = s_0(r) + s(r,z,t)\,. \quad (18\mathrm{d-f})$$

Since the mean flow properties, that appear as coefficients in the linearisation, depend on r but not (z,t), the Fourier transform is made (19) with frequency ω and axial wavenumber k,

$$f(r,z,t) = \int_{-\infty}^{+\infty} \mathrm{d}k \int_{-\infty}^{+\infty} \mathrm{d}\omega e^{\mathrm{i}(kx-\omega t)} \tilde{f}(r,k,\omega)\,; \quad (19)$$

for example the linearised material derivative (13) leads (20a) to the frequency (20b) Doppler shifted by the axial mean flow,

$$\mathrm{d}/\mathrm{d}t \to -\mathrm{i}\omega_* : \quad \omega_* = \omega - kU\,. \quad (20\mathrm{a,b})$$

Substituting (18a–f) in (1,2a–c,3,4) and linearising leads to

$$\mathrm{i}\omega_* r\tilde{\rho} - \rho_0(r\tilde{v}_r)' - \mathrm{i}\rho_0 k r\tilde{v}_z = 0\,, \quad (21a)$$

$$\mathrm{i}\rho_0\omega_*\tilde{v}_r + 2\Omega\rho_0\tilde{v}_\varphi + \Omega^2 r\tilde{\rho} - \tilde{p}' = 0\,, \quad (21b)$$

$$\mathrm{i}\omega_*\tilde{v}_\varphi - 2\Omega\tilde{v}_r = 0\,, \quad (21c)$$

$$\rho_0\omega_*\tilde{v}_z - k\tilde{p} = 0\,, \quad (21d)$$

$$\mathrm{i}\omega_*\tilde{s} = s_0'\tilde{v}_r = C_P\frac{\Omega^2}{c_0^2} r\tilde{v}_r\,, \quad (21e)$$

$$\tilde{p} = c_0^2\tilde{\rho} + \beta_0\tilde{s}\,. \quad (21f)$$

The last equation (21f) follows from linearisation of (4),

$$\mathrm{i}\omega_*(\tilde{p} - c_0^2\tilde{\rho} - \beta_0\tilde{s}) = \tilde{v}_r(p_0' - c_0^2\rho_0' - \beta_0 s_0') = 0\,, \quad (22)$$

using (15a) and (17b). The energy equation (3) simplifies to (23a) for a perfect gas (7a),

$$\frac{P}{R}\frac{\mathrm{D}S}{\mathrm{d}t} = 0 : \quad p_0\frac{\mathrm{d}s_0}{\mathrm{d}t} = 0\,, \quad 0 = (p+p_0)\frac{\mathrm{D}(s+s_0)}{\mathrm{d}t} - p_0\frac{\mathrm{d}s_0}{\mathrm{d}t}\,, \quad (23\mathrm{a-c})$$

implying that: (i) the mean flow is isentropic (23b), that is consistent (13) with the entropy being a function of the radius (14b); (ii) subtracting the mean state (23b) from the exact energy equation (23a) leads to (23c) that is linearised (23d),

$$0 = p_0\frac{\mathrm{D}s}{\mathrm{d}t} + p\frac{\mathrm{D}s_0}{\mathrm{d}t} + p_0\frac{\mathrm{D}s_0}{\mathrm{d}t} - p_0\frac{\mathrm{d}s_0}{\mathrm{d}t} = p_0\frac{\mathrm{d}s}{\mathrm{d}t} + p_0\left(\boldsymbol{V}\cdot\boldsymbol{\nabla}s_0\right)\,; \quad (23d)$$

(iii) from (23d) follows (23e),

$$\frac{\mathrm{d}s}{\mathrm{d}t} = -\left(\boldsymbol{V}\cdot\boldsymbol{\nabla}s_0\right)\,, \quad \mathrm{i}\omega_*\tilde{s} = s_0'\tilde{v}_r\,, \quad (23\mathrm{e,f})$$

proving (23f)≡(21e).

2.3 Wave equation for the radial velocity and polarization relations

Of the six variables in (21a–f) four $(\tilde{v}_r, \tilde{v}_\varphi, \tilde{\rho}, \tilde{s})$ are expressible (21d,c,e,a) in terms of $(\tilde{p}, \tilde{v}_r)$,

$$\tilde{v}_z = \frac{k}{\rho_0\omega_*}\tilde{p}\,, \quad \tilde{v}_\varphi = -\mathrm{i}\frac{2\Omega}{\omega_*}\tilde{v}_r\,, \quad \tilde{s} = -\mathrm{i}C_P\frac{\Omega^2}{c_0^2\omega_*} r\tilde{v}_r\,. \quad (24\mathrm{a-c})$$

$$\tilde{\rho} = -\mathrm{i}\frac{\rho_0}{\omega_* r}(r\tilde{v}_r)' + \frac{k^2}{\omega_*^2}\tilde{p}\,. \tag{24d}$$

Substituting (24c,d) in (21f) leads to

$$\mathrm{i}\tilde{p}\left(\omega_* - k^2 c_0^2/\omega_*\right) = \rho_0\left(\Omega^2 r + c_0^2/r\right)\tilde{v}_r + \rho_0 c_0^2 \tilde{v}_r'\,, \tag{25}$$

the pressure in terms of the radial velocity spectrum.

Substituting (24b,d) in (21b) leads to a relation between $\tilde{p}$ and $\tilde{v}_r$ distinct from (25), namely

$$\mathrm{i}\rho_0\left[\left(\omega_*^2 - 5\Omega^2\right)\tilde{v}_r - \Omega^2 r\tilde{v}_r'\right] = \omega_*\tilde{p}' - \frac{k^2\Omega^2 r}{\omega_*}\tilde{p}\,. \tag{26}$$

Substituting $\tilde{p}$ from (25) in (26) leads to the acoustic-vortical-entropy wave equation for the radial velocity perturbation spectrum,

$$c_0^2\tilde{v}_r'' + A\tilde{v}_r' + B\tilde{v}_r = 0\,, \tag{27}$$

with coefficients

$$X \equiv 1 - k^2 c_0^2/\omega_*^2 : \quad A = c_0^2/r + X\left[c_0^2/X\right]'\,, \tag{28a, b}$$

$$B = \left(\omega_*^2 - 5\Omega^2\right)X - k^2\Omega^2\left(\Omega^2 r^2 + c_0^2\right)/\omega_*^2 + X\left[\left(\Omega^2 r + c_0^2/r\right)/X\right]'\,. \tag{28c}$$

In conclusion the axisymmetric compressive, vortical, non-isentropic perturbations of a uniform axial flow with rigid body swirl (12a), with frequency ω and axial wavenumber k, lead (19) to the acoustic-vortical-entropy wave equation (27) with coefficients (28a–c) satisfied by the radial velocity perturbation spectrum. The other wave variables are specified by the following polarization relations: (i–iii) the pressure (25), entropy (24c) and azimuthal velocity (24b) perturbation spectra; (iv–v) the axial velocity (24a) and mass density (24d) perturbation spectra lead, by (25), respectively to (29a) and (29b),

$$\tilde{v}_z = -\mathrm{i}k\left[\left(\Omega^2 r + c_0^2/r\right)\tilde{v}_r + c_0^2\tilde{v}_r'\right]/\left(\omega_*^2 - k^2 c_0^2\right)\,, \tag{29a}$$

$$\mathrm{i}\tilde{\rho}/\rho_0 = \tilde{v}_r'/\omega_* + \tilde{v}_r/(\omega_* r) + k^2\left[\left(\Omega r + c_0^2/r\right)\tilde{v}_r + c_0^2\tilde{v}_r'\right]/\left(\omega_*^3 - k^2 c_0^2\omega_*\right)\,. \tag{29b}$$

The temperature perturbation spectrum follows from the equation of state (7a),

$$R\tilde{T} = \frac{\tilde{p}}{\rho_0} - \frac{p_0}{\rho_0^2}\tilde{\rho} = \frac{\mathrm{i}c_0^2}{\omega_*\gamma}\left(\tilde{v}_r' + \tilde{v}_r/r\right) - \mathrm{i}\frac{\omega_* - k^2 c_0^2/\gamma\omega_*}{\omega_*^2 - k^2 c_0^2}\left[\left(\Omega^2 r + c_0^2/r\right)\tilde{v}_r + c_0^2\tilde{v}_r'\right]\,, \tag{30a, b}$$

using (29b) and (25).

3 Monotonic and oscillatory inner and outer solutions

The acoustic-vortical-entropy wave equation with zero axial wavenumber is solved exactly as ascending (Subsection 3.2) and descending (Subsection 3.3) power series of the radius that converge respectively inside and outside a critical radius, where the isothermal swirl Mach number is unity. This specifies the separation condition between oscillatory and monotonic dependence of the radius of the AVE wave perturbation of the compressible, vortical, non-isentropic mean flow: (i) near the axis oscillatory solutions correspond to the frequency larger than the vorticity (Subsection 3.1); (ii) at infinity the condition for oscillatory solutions is opposite, that is the vorticity must exceed the frequency (Subsection 3.3).

3.1 Condition separating oscillatory from monotonic radial dependences

If the axial wavenumber is not zero, the vanishing of (28a) introduces singularities in the AVE wave equation (27). The present paper concentrates in the simpler case of zero axial wavenumber (31a), that is neglecting axial dependence, there is (20b) no Doppler shift (31b) and the coefficients of the wave equation (28a–c) simplify respectively to (31d–f),

$$k = 0\,,\ \omega_* = \omega\,,\ (c_0^2)' = \gamma\Omega^2 r\,, X = 1 : \quad A = c_0^2/r + (c_0^2)' = \gamma\Omega^2 r + c_0^2/r\,, \tag{31a - e}$$

$$B = \omega^2 - 5\Omega^2 + \left(\Omega^2 r + c_0^2/r\right)' = \omega^2 - 4\Omega^2 + \gamma\Omega^2 - c_0^2/r^2 \,, \tag{31f}$$

where the radial dependence of the sound speed (16c) was used (31c). Thus the acoustic-vortical-entropy wave equation (27) for (31a–f) an axisymmetric mode of frequency ω simplifies to

$$c_0^2 \tilde{v}_r'' + \left(\gamma\Omega^2 r + c_0^2/r\right) \tilde{v}_r' + \left[\omega^2 + (\gamma - 4)\Omega^2 - c_0^2/r^2\right] \tilde{v}_r = 0 \,. \tag{32}$$

The radial dependence of the sound speed (16b) is quadratic (33a),

$$[c_0(r)]^2 = c_{00}^2 \left[1 + (r/r_0)^2\right] \,, \quad r_0 = (c_{00}/\Omega)\sqrt{2/\gamma} \,, \tag{33a, b}$$

with reference radius (33b). Substituting (33b) in the wave equation (32) leads to

$$r^2 \left(1 + r^2/r_0^2\right) \tilde{v}_r'' + r \left(1 + 3r^2/r_0^2\right) \tilde{v}_r' + \left\{\left[(\omega/c_{00})^2 + (1 - 8/\gamma)/r_0^2\right] r^2 - 1\right\} \tilde{v}_r = 0 \,. \tag{34}$$

Using (31a) and (33a,b), the remaining wave variables are the azimuthal velocity (24b), mass density (29b), temperature (30a), entropy (24c) and pressure (25) specified respectively by (35a–e),

$$\tilde{v}_\varphi = -\mathrm{i}\frac{2\Omega}{\omega}\tilde{v}_r \,, \quad \tilde{\rho} = -\mathrm{i}(\rho_0/\omega)\left(\tilde{v}_r' + \tilde{v}_r/r\right) \,, \quad \tilde{T}/T_0 = \left[(\gamma/c_0^2)\tilde{p} - \tilde{\rho}\right]/\rho_0 \,, \tag{35a - c}$$

$$\tilde{s} = -\mathrm{i}\frac{2}{\omega}\frac{C_V r \tilde{v}_r}{r^2 + r_0^2} \,, \quad \tilde{p} = -\mathrm{i}\frac{\rho_0\gamma\Omega^2}{2\omega}\left[\left(r + 2r/\gamma + r_0^2/r\right)\tilde{v}_r + \left(r^2 + r_0^2\right)\tilde{v}_r'\right] \,, \tag{35d, e}$$

in terms of the radial velocity perturbation spectrum.

The adiabatic exponent for a perfect gas is given by (36b) where (36a) is the number of degrees of freedom of a molecule,

$$N = 3, 5, 6 : \quad \gamma = 1 + \frac{2}{N} = \frac{5}{3}, \frac{7}{5}, \frac{4}{3} \,, \tag{36a, b}$$

namely: (i) three for monoatomic gas; (ii) five for a diatomic gas or polyatomic gas with molecules in a line; (iii) six for a three-dimensional polyatomic molecule. The reference radius (33b) corresponds to a ratio of the azimuthal velocity of the mean flow to the sound speed on axis given by

$$\frac{r_0\Omega}{c_{00}} = \sqrt{\frac{2}{\gamma}} = \sqrt{\frac{2N}{N+2}} = \sqrt{\frac{6}{5}}, \sqrt{\frac{10}{7}}, \sqrt{\frac{3}{2}} \,, \tag{37}$$

that is of order unity and plays the role of swirl Mach number at the axis, bearing in mind that the sound speed (33a,b) is not constant. Using the sound speed (33a) at the critical radius (38a) leads to (38b),

$$c_0(r_0) = c_{00}\sqrt{2} : \quad r_0\Omega = \frac{c_0(r_0)}{\sqrt{\gamma}} = \sqrt{RT_0(r_0)} = \bar{c}_0(r_0) \,, \tag{38a, b}$$

showing that the critical radius corresponds to azimuthal velocity equal to the isothermal sound speed, that is isothermal swirl Mach number unity. Since vortical modes are transversal and hence incompressible, the relevant sound speed and Mach number are isothermal. If the radius is small compared with the reference radius (39a), that is for small swirl isothermal Mach number, the wave equation (34) simplifies to (39b),

$$r^2 \ll r_0^2 : \quad r^2\tilde{v}_r'' + r\tilde{v}_r' + \left(\chi^2 r^2 - 1\right)\tilde{v}_r = 0 \,, \tag{39a, b}$$

that is a Bessel equation of order unity with radial wavenumber (40a),

$$\chi \equiv \kappa/r_0 \,, \quad \kappa^2 = \bar{\omega}^2 + 1 - 8/\gamma \,, \quad \bar{\omega} \equiv \omega r_0/c_{00} \,, \tag{40a - c}$$

where (40b) is the dimensionless radial wavenumber involving the dimensionless frequency (40c).

The Bessel equation has oscillatory solutions for real wavenumber and monotonic increasing solutions for imaginary wavenumber. Although the preceding result was obtained only for small radius (39a), it will be extended in the sequel (Subsections 3.2 and 3.3) to all values of the radial

distance. Thus the condition specifying wave fields with oscillatory dependence on the radius (41a) is expressed in terms of the dimensionless frequency (40b),

$$\kappa^2 > 0 \; : \quad \frac{\omega r_0}{c_{00}} > \sqrt{\frac{8}{\gamma} - 1} = \sqrt{\frac{7N-2}{N+2}} = \sqrt{\frac{19}{5}, \frac{33}{7}, 5}\,. \tag{41a, b}$$

Using (33b) the condition for radially oscillatory AVE waves is written in terms of the angular velocity,

$$\omega > \frac{c_{00}}{r_0}\sqrt{\frac{8}{\gamma} - 1} = \Omega\sqrt{\frac{\gamma}{2}\left(\frac{8}{\gamma} - 1\right)} = \Omega\sqrt{4 - \frac{\gamma}{2}} = \Omega\sqrt{\frac{7}{2} - \frac{1}{N}} = \Omega\sqrt{\frac{19}{6}, \frac{33}{10}, \frac{10}{3}}\,. \tag{42}$$

Using the sound speed (38a) at the reference radius the oscillatory condition (41b) becomes

$$\frac{\omega r_0}{c_0(r_0)} = \frac{\omega r_0}{c_{00}\sqrt{2}} > \sqrt{\frac{4}{\gamma} - \frac{1}{2}} = \sqrt{\frac{8-\gamma}{2\gamma}} = \sqrt{\frac{7N-2}{2N+4}} = \sqrt{\frac{19}{10}, \frac{33}{14}, \frac{5}{2}}\,. \tag{43}$$

Bearing in mind that the vorticity is twice the angular velocity (12b) the oscillatory condition (42) becomes

$$\frac{\omega}{\varpi} = \frac{\omega}{2\Omega} > \sqrt{1 - \frac{\gamma}{8}} = \sqrt{\frac{7}{8} - \frac{1}{4N}} = \sqrt{\frac{7N-2}{8N}} = \sqrt{\frac{19}{24}, \frac{33}{40}, \frac{5}{6}} \equiv \mu\,. \tag{44}$$

Of the four forms of the oscillatory condition (41b), (42), (43) and (44) the last is independent of the geometry and may be the most general: a compressible, vortical, non-isentropic flow has perturbations with oscillatory dependence on the radial distance if the frequency is larger than the peak vorticity ϖ multiplied by the factor μ in (44). The spatial growth of perturbations of acoustic-vortical waves (49; 50) is comparable to the temporal growth (51) as an indicator of instability. Thus the oscillatory condition excluding monotonic growth of perturbations could be equivalent to a stability condition for the mean flow. This conjecture can be applied (Figure 1) to combustion stability in a confined space: (i) if the natural frequencies exceed the product $\mu\varpi$ there is (Figure 1a) stability, and only the fundamental frequency needs to be considered $\omega_1 > \mu\varpi$; (ii) if the fundamental frequency and other modes lie below $\mu\varpi$ those modes lead to instability (Figure 1b). The passage from stable to the unstable case could be due to: (i) increasing the

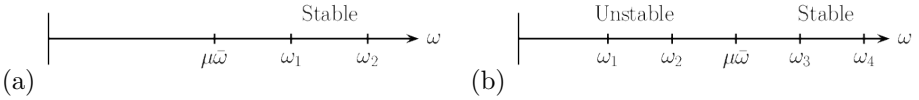

Figure 1: The compressible, vortical, non-isentropic flow is stable if the peak vorticity multiplied by (44) is less than the fundamental frequency (Figure 1a) and unstable otherwise (Figure 1b).

vorticity of the mean flow, e.g. to achieve better mixing for 'lean' fuel saving combustion; (ii) increasing the size of the enclosure, so that the natural frequencies reduce, and fall below $\mu\varpi$. The remark (i) agrees with the observation that lean combustion tends to be unstable; the remark (ii) agrees with the observation that larger rocket motors are more prone to large amplitude oscillations. The stability criterion

$$\omega_1 > \mu\varpi_{max}\,, \quad \mu = 0.890, 0.908, 0.913\,, \tag{45a, b}$$

that the fundamental frequency must be larger than the peak vorticity times the factor (44) can be tested for more complex geometries using numerical codes. It has a simple interpretation: (i) acoustic modes with frequency ω are stable; (ii) vortical modes with vorticity ϖ are unstable; (iii) there is stability if the acoustic modes predominate $\omega > \varpi$; (iv) there is instability if the vortical modes predominate $\varpi > \omega$. The factor (44) involving the adiabatic exponent appears because the vortical modes are incompressible and the acoustic modes are adiabatic and thus the ratio of frequency to vorticity is close to but not exactly unity. The stability condition (45a,b) was established from the AVE wave equation (39b) for small radius (39a). Next it will be shown that the equivalent condition for AVE waves with oscillatory radial dependence is not restricted to small radius (39a) and applies to any radial distance smaller than the critical radius.

3.2 Regular and logarithmic solutions inside the critical radius

The independent variable is chosen to be the square of the radius divided by the reference radius (46a),

$$s \equiv (r/r_0)^2 = \frac{\Omega^2 \gamma r^2}{2c_{00}^2} = \frac{\Omega^2 \gamma r^2}{[c_0(r_0)]^2} = \frac{\Omega^2 r^2}{RT_0(r_0)} \,, \quad \tilde{v}_r(r,\omega) = J(s,\kappa) \,, \tag{46a, b}$$

that is unity at the radial distance of unit isothermal swirl Mach number. The acoustic-vortical-entropy wave equation (34) becomes

$$s^2(1+s)J'' + s(1+2s)J' + [(\kappa^2 s - 1)/4]J = 0 \,, \tag{47}$$

that involves as parameter only the radial wavenumber (40b), that includes all compressibility, vorticity and non-isentropic effects. The zero or infinite values of the coefficient of the highest order derivative (48a) determine the singularities of the differential equation (47), namely (48b),

$$s^2(1+s) = 0 \,, \infty \, : \qquad s = 0 \,, \infty \,, -1 \,, \quad r = 0 \,, \infty \,, \pm i r_0 \,. \tag{48a - c}$$

From the location (Figure 2) of the singularities (48c) it follows that: (i) the singularities at the origin $r = 0$ and infinity $r = \infty$ lead to a pair of solutions respectively in ascending $W_\pm$ and descending $W^\pm$ powers of the radius; (ii) the singularities at $|r| = r_0$ imply that the ascending series solution converges for $|r| < r_0$ and the descending series solution converges for $|r| > r_0$; (iii) even if either or both series do not converge at the circle of convergence, a pair of solutions $W_{1,2}$ around the critical radius overlaps with the first two and allows their matching (Figure 2). In this way the exact solution of the AVE wave equation can be obtained for all radial distances, as shown next (Subsections 3.2 and 3.3 and Section 4).

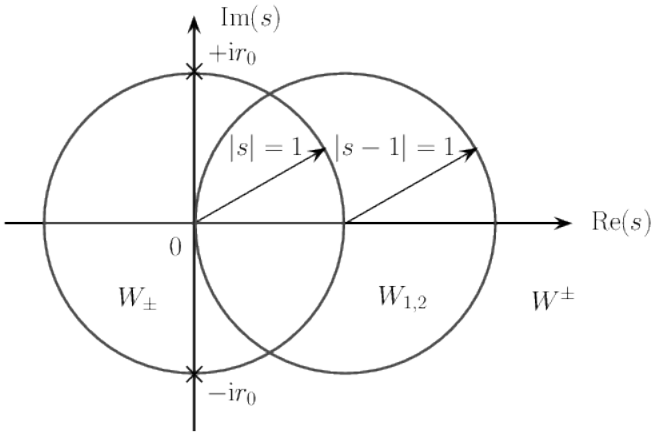

Figure 2: The AVE wave equation (34) rewritten (47) in terms of the variables (46a,b) has singularities at (48a–c) implying that: (i) the pair of solutions $W_\pm$ around the singularity at the origin are series of ascending powers of the radius that converge inside the critical layer $0 \leq r < r_0$; (ii) the pair of solutions $W^\pm$ around the singularity at infinity are series of descending powers of the radius that converge outside the critical layer $r_0 < r \leq \infty$; (iii) the two pairs of solutions (i) and (ii) are matched by a third pair $W_{1,2}$ around the critical radius that are power series of $(r/r_0)^2 - 1$ with region of convergence overlapping with those of $W_\pm$ and $W^\pm$.

The origin is a regular singularity (59) of the differential equation (47), and thus at least one solution exists as a Frobenius-Fuchs series of ascending powers of the radius,

$$|s| < 1 \, : \qquad J_\sigma(s,\kappa) = \sum_{n=0}^{\infty} a_n(\sigma) s^{n+\sigma} \,, \tag{49a, b}$$

with index σ and coefficients to be determined. Substituting (49b) in (47) leads to

$$\left[(n+\sigma)^2 - 1/4\right] a_n(\sigma) = -\left[(n+\sigma-1)(n+\sigma) + \kappa^2/4\right] a_{n-1}(\sigma) \,. \tag{50}$$

Setting (51a) leads to the indicial equation (51b) with roots (51c),

$$n = 0 : \qquad (\sigma^2 - 1/4)a_0(\sigma) = 0 \Rightarrow \sigma = \pm 1/2 \,. \tag{51a-c}$$

The solution corresponding to the upper root (52a) has recurrence formula (50) for the coefficients (52b),

$$\sigma = 1/2 : \quad a_n(1/2) = -\frac{(n-1/2)(n+1/2)+\kappa^2/4}{(n+1/2)^2-1/4} a_{n-1}(1/2) = \\ = -\frac{n^2+(\kappa^2-1)/4}{n(n+1)} a_{n-1}(1/2) \,. \tag{52a,b}$$

This double recurrence formula specifies explicitly the coefficients (53b),

$$a_0(1/2) = 1 : \qquad a_n(1/2) = \frac{(-)^n}{n!(n+1)!} \prod_{m=1}^{n} \left[m^2 + (\kappa^2-1)/4 \right] \equiv a_n^+ \,, \tag{53a,b}$$

where the first coefficient may be set to unity (53a) because the solution is valid to within a multiplying constant. Substitution of (52a;53b) in (49a,b;46a,b) specifies the radial velocity perturbation,

$$r < r_0 : \qquad W_+(r,\kappa) = \sum_{n=0}^{\infty} a_n^+ (r/r_0)^{2n+1} = J_{1/2}(s,\kappa) \,, \tag{54a,b}$$

that vanishes at the origin like $O(r)$, in agreement with the Bessel function $J_1(\kappa r)$ that is the solution of (39b) for small radius. The differential equation (47) can be transformed to the Gaussian hypergeometric type, leading to the solution (54a,b) in an alternative way (Subsection 4.1).

The indexes (51c) differ by an integer (55a) and thus the second solution (60) is given by (55b),

$$\sigma_+ - \sigma_- = 1 : \quad W_-(r,\kappa) = Y_{-1/2}(s,\kappa) = \lim_{\sigma \to -1/2} \frac{\partial}{\partial \sigma} \left[(\sigma + 1/2) J_\sigma(s,\kappa) \right] \,. \tag{55a,b}$$

The solution (55b) is a function of the second kind,

$$Y_-(s,\kappa) = \log s \sum_{n=0}^{\infty} a_n^+ s^{n-1/2} + \sum_{n=0}^{\infty} a_n^- s^{n-1/2} \,, \tag{56}$$

that consists of a logarithmic singularity multiplied by a function of the first kind plus a complementary function that has a power type singularity $s^{-1/2}$. The notation (J,Y) is used for the solutions regular (49b) and singular (56) at the origin, as for Bessel and Neumann functions respectively, of which they are an extension for (39a) to $r < r_0$. The coefficients a_n^- follow by substitution in (55b) of (49b) with the recurrence formula (50) leading to (57),

$$n \geq 1 : \qquad a_n^- = a_n^+ \left[\psi(n+1+\nu/2) + \psi(n+1-\nu/2) - \psi(n+2) - \psi(n) \right] \,, \tag{57a,b}$$

where appears the ψ function (61; 17) and (58b),

$$\nu \equiv \sqrt{1-\kappa^2} \,; \quad a_0^- = -(\kappa^2-1)(\kappa^2-3)/16 \,, \tag{58a,b}$$

The exception to (57a,b) is the coefficient (58b) as can be confirmed in Subsection 4.1. The solution of the second kind,

$$r < r_0 : \qquad W_-(r,\kappa) = 2\log(r/r_0) \sum_{n=0}^{\infty} a_n^+ (r/r_0)^{2n+1} + \sum_{n=0}^{\infty} a_n^- (r/r_0)^{2n-1} \,, \tag{59a,b}$$

consists of two terms: (i) the logarithmic singularity in the first term on the r.h.s. of (59) is dominated by the factor r/r_0 as $r \to 0$, so this term vanishes at the origin; (ii) the second term on the r.h.s. of (59) has a singularity r_0/r at the origin with coefficient (58b). This can be confirmed from the Gaussian hypergeometric function of the second kind (Subsection 4.1). The general integral is a linear combination of the two solutions:

$$0 \leq r < r_0 : \qquad \tilde{v}_r(r,\omega) = C_+ W_+(r,\kappa) + C_- W_-(r,\kappa) \,, \tag{60a,b}$$

where $C_\pm$ are arbitrary constants. In the case of a cylinder of radius $r_1 \geq r \geq 0$, the solution finite on axis is obtained setting $C_- = 0$ in (60b), and consists only of the function of first kind (54a,b). The regular (54a,b) and singular (60a,b) solutions correspond to Gaussian hypergeometric functions respectively of the first and second kinds (Subsection 4.1).

3.3 Asymptotic series outside the critical radius

The solution (60b) is valid inside the reference radius (60a), and the solution valid outside is obtained using the inverse (61a) of the variable (46a),

$$\zeta = \frac{1}{s} = (r_0/r)^2 \;, \quad \tilde{v}_r(r,\omega) = J(s,\kappa) = H(\zeta,\kappa)\,, \tag{61a, b}$$

leading from (47) to the differential equation

$$\zeta^2(\zeta+1)H'' + \zeta^2 H' + [(\kappa^2-\zeta)/4]H = 0\,. \tag{62}$$

The point at infinity $r = \infty$ corresponds to the origin $\zeta = 0$ of (61a), that is a regular singularity of the differential equation (62) implying the existence of a Frobenius-Fuchs series solution,

$$\zeta < 1 \;: \qquad H_\vartheta(\zeta,\kappa) = \sum_{n=0}^{\infty} b_n(\vartheta)\zeta^{n+\vartheta}\,, \tag{63a, b}$$

that corresponds to a descending power series of the radius,

$$r > r_0 \;: \quad \tilde{v}_r(r,\omega) = \sum_{n=0}^{\infty} b_n(\vartheta)(r_0/r)^{2n+2\vartheta}\,. \tag{64a, b}$$

Substitution of (63b) in (62) leads to the recurrence formula for the coefficients:

$$\left[(n+\vartheta)(n+\vartheta-1)+\kappa^2/4\right] b_n(\vartheta) = -\left[(n+\vartheta-1)^2 - 1/4\right] b_{n-1}(\vartheta)\,. \tag{65}$$

Setting (66a) leads to the indicial equation (66b),

$$n = 0 \;: \qquad (\vartheta^2 - \vartheta + \kappa^2/4)b_0(\vartheta) = 0 \;\Rightarrow 2\vartheta_\pm = 1 \pm \sqrt{1-\kappa^2} = 1 \pm \nu\,, \tag{66a - c}$$

that has roots (66c) where appears (58a). The corresponding recurrence formula for the coefficients is

$$b_n(\vartheta_\pm) = -\frac{(n \pm \nu/2 - 1/2)^2 - 1/4}{(n \pm \nu/2 + 1/2)(n \pm \nu/2 - 1/2) + \kappa^2/4} b_{n-1}(\vartheta_\pm). \tag{67}$$

The double recurrence formula (67) allows explicit calculation of the coefficients,

$$b_0(\vartheta_\pm) = 1 \;: \qquad b_n(\vartheta_\pm) = (-)^n \prod_{m=1}^{n} \frac{(2m \pm \nu)(2m \pm \nu - 2)}{(2m \pm \nu)^2 - 1 + \kappa^2}\,. \tag{68a, b}$$

The corresponding solutions (64a,b) are

$$r > r_0 \;: \qquad W^\pm(r,\kappa) = \sum_{n=0}^{\infty} b_n^\pm (r_0/r)^{2n+1\pm\nu} = H_{\vartheta_\pm}(\zeta,\kappa)\,, \tag{69a, b}$$

are linearly independent for $\nu \neq 0$ and will be checked in Subsection 4.2. The general integral is their linear combination,

$$r > r_0 \;: \qquad \tilde{v}_r(r,\omega) = C^+ W^+(r,\kappa) + C^- W^-(r,\kappa)\,, \tag{70a, b}$$

involving the arbitrary constants $C^\pm$. If $\nu > 1$, that is for $\kappa^2 < 0$ or imaginary κ in (58a), the solution W^- diverges (69b) as $r \to \infty$, and must be suppressed setting $C^- = 0$, leaving only the solution W^+. The latter would also diverge as $r \to \infty$ if $\mathrm{Re}(\nu) < -1$, but this is not possible since

ν in (58a) is either imaginary for $\kappa^2 > 1$ or $\nu > -1$ for $\kappa^2 \leq 1$. Thus the solution W^+ is always bounded at infinity. The two solutions (69b) are oscillatory (71b) for $\kappa^2 > 1$ or imaginary ν,

$$\nu = \mathrm{i}|\nu| \; : \qquad (r_0/r)^{1\pm\nu} = (r_0/r)^{1\pm\mathrm{i}|\nu|} = (r_0/r)\exp\left[\pm\mathrm{i}|\nu|\log(r_0/r)\right] , \tag{71a, b}$$

and vanish at infinity. For $0 < \kappa^2 < 1$ then $|\nu_\pm| < 1$ in (58a) and both solutions (69a,b) converge. In conclusion: (i) for imaginary radial wavenumber $\kappa^2 < 0$, that is the opposite of (41a), there is monotonic radial growth inside the critical radius, and outside the critical radius W^- in (69b) diverges as $r \to \infty$ since $|\nu| > 1$ in (58a); (ii) for $\kappa^2 > 1$ that satisfies (41a) there is oscillation inside the critical radius and since ν is imaginary in (58a) the solutions outside the critical radius (71a,b) are oscillatory and decaying; (iii) for $0 < \kappa^2 < 1$ the radial oscillation inside the critical radius remains (41a) and since $|\nu| < 1$ in (58a) the solutions (69a,b) outside the critical radius are monotonic and decaying. The oscillatory condition $\kappa^2 > 0$ in (41a) corresponds to (41b,42,43,44) and the monotonic condition $\kappa^2 < 0$ to the reverse. The condition (72a) of oscillatory waves at infinity (71a,b) corresponds (40b,c) to (72b),

$$\kappa^2 > 1 \; : \qquad \bar{\omega} = \frac{\omega r_0}{c_{00}} > \sqrt{\frac{8}{\gamma}} = \sqrt{\frac{8N}{N+2}} = \sqrt{\frac{24}{5}, \frac{40}{7}, 6} \, . \tag{72a, b}$$

The comparison of the inner acoustically dominated and outer vorticity dominated solutions, respectively in ascending and descending power series of the radius, valid inside and outside the critical radius raises the questions (i) of convergence at (Subsection 5.1) and (ii) of matching (Section 4) across the critical radius. This matching can be addressed via hypergeometric functions (Section 4).

4 Matching of inner and outer solutions across the critical layer

The AVE wave equation (Section 3) can be transformed to the Gaussian hypergeometric type: (i) confirming the inner (Subsection 3.2 and 4.1) and outer (Subsection 3.3 and 4.2) solutions respectively inside and outside the critical layer; (ii) providing the matching of (i) accross the critical layer thus specifying the AVE wave field in all space.

4.1 Transformation to a Gaussian hypergeometric differential equation

The differential equation (47) was solved using directly the Frobenius-Fuchs method since this is the quickest way to obtain the acoustic-vortical-entropy wave field (54a,b;53a,b). The solutions can be obtained alternatively in terms of Gaussian hypergeometric functions by means of changes of dependent and independent variables indicated next. The change of dependent variable (73a) in (47) leads to (73b),

$$J(s) = s^\alpha K(s) \; : \tag{73a}$$

$$s^2(1+s)K'' + s[1 + 2\alpha + 2(1+\alpha)s]K' + [(\alpha^2 + \alpha + \kappa^2/4)s + \alpha^2 - 1/4]K = 0 \, , \tag{73b}$$

where the constant α may be chosen at will. Choosing (74a) allows (73b) to be divided through s, depressing the degree of the coefficients from three in (73b) to two in (74b),

$$\alpha = \frac{1}{2} \; : \quad s(1+s)K'' + (2+3s)K' + [(\kappa^2+3)/4]K = 0 \, . \tag{74a, b}$$

A further change of independent variable (75a,b) leads to (75c),

$$u = -s \, , \; K(s) = Q(u) \; : \quad u(1-u)Q'' + (2-3u)Q' - [(\kappa^2+3)/4]Q = 0 \, . \tag{75a - c}$$

The latter is a Gaussian hypergeometric differential equation (62),

$$u(1-u)Q'' + [C - (A+B+1)u]Q' - ABQ = 0 \, , \tag{76}$$

with parameters satisfying (77a-c),

$$C=2\,,\;A+B=2\,,\;AB=\frac{\kappa^2+3}{4}\;:\quad A,B=1\pm\frac{1}{2}\sqrt{1-\kappa^2}=1\pm\frac{\nu}{2}\,, \tag{77a-d}$$

and implying (77d).

Since $C=2$, there is only one solution without logarithmic singularity at $u=0$, namely the Gaussian hypergeometric function of the first kind,

$$Q_+(u)=F(A,B;C;u)=1+\sum_{n=1}^{\infty}\frac{u^n}{n!}\prod_{m=1}^{n}\frac{(A+m-1)(B+m-1)}{(C+m-1)}\,, \tag{78}$$

where was used the hypergeometric series. Substitution of (77a-c,75a,74a,73a,46a) leads to

$$\begin{aligned}\tilde{v}_r^1 &= \frac{r}{r_0}F\left(A,B;2;-\frac{r^2}{r_0^2}\right)\\ &= \frac{r}{r_0}\left\{1+\sum_{n=1}^{\infty}\frac{(r/r_0)^{2n}}{n!(n+1)!}(-)^n\prod_{m=0}^{n}\left[(m-1)^2+2(m-1)+\frac{\kappa^2+3}{4}\right]\right\}\\ &= \frac{r}{r_0}\left[1+\sum_{n=1}^{\infty}\frac{(r/r_0)^{2n}}{n!(n+1)!}(-)^n\prod_{m=0}^{n}\left(m^2+\frac{\kappa^2-1}{4}\right)\right]=W_+(r,\kappa)\,,\end{aligned} \tag{79}$$

that coincides with (54b,53b). Since the Gaussian hypergeometric differential equation (75c) has integer third parameter (77a), the pair of linearly independent solutions consists of: (i) a function of the first kind (79) with leading power term; (ii) a functions of the second kind with logarithmic singularity considered next (Subsection 4.2).

4.2 Power and logarithmic singularities of the functions of the first and second kind

The solution with logarithmic singularity at the origin is a function of the second kind (62; 63),

$$Q_-(u)=G(A,B;2;u)=F(A,B;2;u)\log u+H(A,B;2;u)\,, \tag{80}$$

with the complementary function

$$\begin{aligned}H(A,B;2;u) &= \frac{A(A-1)B(B-1)}{u}+\sum_{n=1}^{\infty}\frac{u^n}{n!}\left[\prod_{m=1}^{n}\frac{(A+m-1)(B+m-1)}{m+1}\right]\\ &\quad\{\psi(A+n)+\psi(B+n)-\psi(n+2)-\psi(n)\}\,,\end{aligned} \tag{81}$$

where the ψ function (61; 17) is the logarithmic derivative of the Gamma function (64; 65). In the case of acoustic-vortical-entropy waves, besides the first solution (79), the second solution is

$$\tilde{v}_r^2(r,\kappa)=2\log(r/r_0)W_+(r,\kappa)+W_*(r,\kappa)\equiv W_-(r,\kappa)\,, \tag{82}$$

including: (i) the regular solution (79) multiplied by a logarithmic singularity; (ii) plus the complementary function (81) that has an algebraic singularity,

$$\begin{aligned}W_*(r,\kappa) &= -\frac{(\kappa^2-1)(\kappa^2+3)}{16}\frac{r_0}{r}+\sum_{n=1}^{\infty}\frac{(-)^n}{n!}\frac{(r/r_0)^{2n}}{(n+1)!}\left[\prod_{m=1}^{n}\left(m^2+\frac{\kappa^2-1}{4}\right)\right]\\ &\quad\{\psi(n+1+\nu/2)+\psi(n+1-\nu/2)-\psi(n+2)-\psi(n)\}\,.\end{aligned} \tag{83}$$

Thus the solution finite on axis consists only of the function of the first kind (79) and holds $|r|<r_0$ inside the critical radius. The solution (80) in terms of the function of the second kind can be written

$$W_-(r,\kappa)=2\log(r/r_0)W_+(r,\kappa)+W_*(r,\kappa)\,, \tag{84}$$

that coincides with (59b) because it consists of the sum of: (i) the function of the first kind (79)≡(54b;53b) multiplied by a logarithmic singularity; (ii) the function of the second kind (83) that coincides with the second term of the r.h.s. of (59b) with coefficient (57b); (iii) the algebraic term r/r_0 in the function of the second kind, corresponding to the first term of the r.h.s. of (83) has (81) has coefficients

$$a_0^- = A(A-1)B(B-1) = \frac{\kappa^2+3}{4}(AB-A-B+1) = \frac{\kappa^2+3}{4}\frac{\kappa^2-1}{4}\,, \tag{85}$$

in agreement with (58b). This completes the pair of solutions of the AVE wave equation inside the critical radius (60a,b).

The wave fields outside the critical radius correspond to the solutions of the hypergeometric equation around the point at infinity (66; 67), namely,

$$Q^+(u) = u^{-A}F(A, A-C+1; A-B+1; 1/u)\,, \tag{86}$$

and another Q^- obtained interchanging (A, B), that is interchanging $\pm\nu$,

$$Q^\pm(u) = (r/r_0)^{1/2\mp\nu}F(1\pm\nu/2, \pm\nu/2; 1\pm\nu; -(r_0/r)^2)\,. \tag{87}$$

The corresponding wave fields are

$$W^\pm(r,\kappa) = \left(\frac{r_0}{r}\right)^{1/2\pm\nu}\left\{1+\sum_{n=1}^{\infty}\frac{(-)^n}{n!}\left(\frac{r_0}{r}\right)^{2n}\prod_{m=1}^{n}\frac{(m\pm\nu/2)(m-1\pm\nu/2)}{m\pm\nu}\right\}, \tag{88}$$

that coincide with (69b,68b) since

$$\begin{aligned}\prod_{m=1}^{n}\frac{(2m\pm\nu)(2m\pm\nu-2)}{(2m\pm\nu)^2-1+\kappa^2} &= \prod_{m=1}^{n}\frac{(2m\pm\nu)(2m\pm\nu-2)}{2m(2m\pm2\nu)+\nu^2-1+\kappa^2}\\ &= \frac{1}{n!}\prod_{m=1}^{n}\frac{(m\pm\nu/2)(m-1\pm\nu/2)}{m\pm\nu}\,,\end{aligned} \tag{89}$$

the coefficients (89) and (68b) are equal. The solutions of the AVE wave equation can be expressed in terms of the Gaussian hypergeometric functions both inside and outside the critical layer (Subsections 3.2–3.3 and 4.1–4.2) and also around the critical layer (Subsection 4.3) showing that the wave field is finite.

4.3 AVE wave field at and around the critical layer

The parameters (77a,b) of the hypergeometric function satisfy $C-A-B=0$, implying (68; 17) that: (i) there is conditional convergence on the boundary of convergence $|s|=1$ or $|r|=r_0$ excluding the point $s=-1=r^2/r_0^2$ or $r=\pm ir_0$; (ii) at this point there is divergence. This shows that the radial velocity perturbation spectrum is finite at the critical radius, as it will be confirmed subsequently (98a,b). This can be confirmed by obtaining the solution of the acoustic-vortical-entropy wave equation around the critical radius. The Gaussian hypergeometric differential equation (76) transforms into itself with different parameters by the changes of independent variable in the Schwartz group,

$$u,\ 1-u,\ \frac{1}{u},\ 1-\frac{1}{u},\ \frac{u-1}{u},\ \frac{u}{u-1}\,, \tag{90}$$

that interchange between themselves the three regular singularities: $u=0,1,\infty$. Since $s>0$ in (46a) and $u<0$ in (75a), the variable (91a) does not exceed unity,

$$\xi \equiv \frac{u}{u-1} = \frac{s}{s+1} = \frac{r^2}{r^2+r_0^2} < 1\,, \quad |r-r_0| < r_0\,, \tag{91a, b}$$

and the corresponding series solution converges for (91b) that is from the origin to twice the critical radius. The solutions of the Gaussian hypergeometric differential equation in terms of the variable (91a) are (62; 66; 67)

$$Q_1(u) = (1-u)^{-A}F(A, C-B; C; u/(u-1))\,, \tag{92a}$$

$$Q_2(u) = u^{1-C}(1-u)^{C-A-1}F(A-C+1, 1-B; 2-C; u/(u-1))\,. \tag{92b}$$

Substituting (77a,d), (91a) and (75a,b; 74a; 73a; 46a,b) leads to

$$W_1(r;\kappa) = (1+r^2/r_0^2)^{-1-\nu/2} F(1+\nu/2, 1+\nu/2; 2; r^2/(r_0^2+r^2)) \,, \tag{93a}$$

$$W_2(r;\kappa) = -(r_0^2/r^2)(1+r^2/r_0^2)^{-\nu/2} F(\nu/2, \nu/2; 0; r^2/(r_0^2+r^2)) \,. \tag{93b}$$

The radial velocity perturbation spectrum is a linear combination of (93a,b),

$$0 < r < 2r_0 \; : \quad W(r;\kappa) = C_1 W_1(r;\kappa) + C_2 W_2(r;\kappa) \,, \tag{94a, b}$$

and is valid (91b) from the axis to twice the critical radius (94a). The value at the critical radius $r = r_0$ corresponds to $\xi = 1/2$ and is finite. Since the AVE wave field has been determined exactly for all values of the radius, it is possible to consider AVE wavemodes in cylindrical or annular ducts for any values of the radii. For example, the wave field up to two critical radii (94a) is given by (94b) where (93b) is singular on axis and must be excluded for a cylindrical duct setting (95a) and leading to (95b),

$$C_2 = 0 \; : \quad W(r;\kappa) = C_1 (1+r^2/r_0^2)^{-1-\nu/2} F(1+\nu/2, 1+\nu/2; 2; r^2/(r^2+r_0^2)) \,. \tag{95a, b}$$

The application of rigid or impedance wall boundary conditions then specifies the eigenvalues and eigenfunctions of AVE modes (Section 5).

5 Velocity, pressure, density, entropy and temperature perturbations

All wave variables, namely the azimuthal velocity, mass density, pressure, temperature and entropy perturbations can be calculated from the radial velocity perturbation (Section 2). The latter satisfies the acoustic-vortical-entropy wave equation whose solution has been obtained (Section 3) as acoustic modes inside and vortical modes outside the critical radius where the isothermal swirl Mach number is unity. It can be shown (Subsection 5.1) that: (i) both solutions converge for the radial velocity perturbation spectrum; (ii) neither solution converges for the pressure perturbation spectrum. The solution around the critical layer (Subsection 4.3) shows that the radial velocity perturbation is finite there and matches the inner and outer solutions (Subsections 4.1 and 4.2). Thus by using the appropriate set from the three pairs of (i) inner, (ii) outer and (iii) middle solutions, the AVE wave fields can be considered inside cylindrical or annular ducts with any radii (Subsection 5.2). The case of a cylinder with critical radius inside with rigid walls at a radius less than twice the critical radius is used (Subsection 5.3) to calculate the natural frequencies and plot the waveforms of acoustic-vortical-entropy waves.

5.1 Divergence of the inner and outer wave fields at the critical radius

The exact inner (outer) solutions of the AVE wave equations converge respectively inside (outside) the critical radius thus specifying the acoustic (vortical) modes; the critical layer, where mode conversion occurs, corresponds to the boundary of convergence of both the inner and outer series solutions. The convergence on the boundary of convergence (17) is specified by the ratio of successive coefficients (53b) [(68b)] in (96) [(97)],

$$\frac{a_{n+1}^+}{a_n^+} = -\frac{(n+1)^2 + (\kappa^2-1)/4}{(n+1)(n+2)} = -\frac{n^2+2n+(\kappa^2+3)/4}{n^2+3n+2} \,, \tag{96}$$

$$\frac{b_{n+1}^\pm}{b_n^\pm} = -\frac{(2n+2\pm\nu)(2n\pm\nu)}{(2n+2\pm\nu)^2-\nu^2} = -\frac{4n^2+4n(1\pm\nu)+\nu^2\pm 2\nu}{4n^2+4n(2\pm\nu)+4(1\pm\nu)} \,. \tag{97}$$

The limit as $n \to \infty$ is

$$\left| \frac{a_{n+1}^+}{a_n^+} \right| = 1 - \frac{1}{n} + O\left(\frac{1}{n^2}\right) = \left| \frac{b_{n+1}^\pm}{b_n^\pm} \right| \,. \tag{98a, b}$$

The combined convergence test (69; 17, p.494) on the boundary of convergence applies to a ratio of terms,

$$\left|\frac{u_{n+1}}{u_n}\right| = 1 - \frac{g}{n} + O\left(\frac{1}{n^2}\right) , \tag{99}$$

and is specified by the value of g. Thus $g = 1$ implying that: (i) both series diverge for $-(r/r_0)^2 = 1$, that is at the singular points $r = \pm i r_0$; (ii) at all other points on the circle of $|-(r/r_0)^2| = 1$ or $|r| = r_0$, the series are conditionally convergent, that is: (ii-1) converge if the order of the terms is not deranged; (ii-2) the series of moduli diverges. Since r is real and positive, the only point on the circle of convergence of physical interest is the critical radius $r = r_0$, where both the inner and outer series for radial velocity perturbation spectrum converge conditionally and can be matched directly. However, the direct matching would also require the pressure perturbation (35e) to be continuous; since it has been shown that $\tilde{v}_r$ is continuous across the critical radius for the direct matching to be possible, $\tilde{v}_r'$ must also be continuous. From (54b) [(69b)] follows the derivative of the radial velocity perturbation for acoustic (vortical) modes inside (outside) the critical radius (100) [(101)],

$$W_+'(r,\kappa) = \frac{1}{r_0}\sum_{n=0}^{\infty}(2n+1)a_n^+(r/r_0)^{2n} , \tag{100}$$

$$[W^{\pm}(r,\kappa)]' = \frac{1}{r_0}\sum_{n=0}^{\infty}(2n+1/2\pm\nu/2)b_n^{\pm}(r/r_0)^{2n\pm\nu} . \tag{101}$$

As $n \to \infty$ both a_n^+ ($b_n^{\pm}$) $\to 1$ tend to unity in (53b) [(68a,b)] and thus the coefficients in (100) [(101)] are $O(n)$, implying divergence on the critical radius $r = r_0$. Thus the pressure perturbation is singular at the critical radius, both for the acoustic and vortical modes, and matching is not possible using directly the inner and outer solutions. The matching can always be performed using the middle solution valid around the critical layer, where the AVE wave field is finite. Thus the failure of the inner and outer solutions to converge at the critical layer is a feature of the representation and not of the wave field, that can be calculated from the alternative representation around the critical layer. This allows the consideration of AVE waves in cylindrical ducts, cavities or annulus with any radii (Subsection 5.2).

5.2 Waves inside or outside a cylinder or in a cylindrical annulus

It has been shown that there are acoustic-vortical-entropy waves finite over the whole range of radial distances leading to (Figure 3) six possibilities: (i–ii) the interior (exterior) of a cylinder inside (outside) the critical radius (Figure 3a) that is using the inner (outer) solution in a cylinder (cylindrical cavity); (iii–iv) a cylindrical annulus either inside or outside the critical radius (Figure 3b); (v–vi) a cylinder (Figure 3c) or cylindrical annulus (Figure 3d) containing the critical layer, using the middle solution alone if the outer radius is less than twice the critical radius, or otherwise matching to the outer solution. The oscillatory or monotonic radial dependence of the wave fields is specified by the inner and outer solutions as indicated in the Table 1. In the case IA of the exterior of a cylinder outside the critical radius (102a) are considered (70b) monotonic vortical modes (102c) that are stable, that is vanish at infinity (69b) if $\nu < 1$ implying (102b),

$$r_0 < r_3 \leq r < \infty \, ; \, 0 < \kappa^2 < 1 : \quad \tilde{v}_r(r,\omega) = C^+W^+(r,\kappa) + C^-W^-(r,\kappa) , \tag{102a-c}$$

and arbitrary constants $C^{\pm}$ are determined by two boundary conditions at $r = r_3$, e.g., pressure and radial velocity. In the case IB of (103a,b), the solution W^- in (69b) is singular at infinity and must be suppressed in (103c),

$$r_0 < r_3 \leq r < \infty \, ; \, \kappa^2 < 0 : \quad \tilde{v}_r(r,\omega) = C^+W^+(r,\kappa) , \tag{103a-c}$$

and the arbitrary constant C^+ is determined by one boundary condition at $r = r_3$. The case IC of an outward propagating vortical wave is possible (104a) for (104b) selecting W^+ in (71b),

$$r_0 < r_3 \leq r < \infty \, ; \, \kappa^2 > 1 : \quad \tilde{v}_r(r,\omega) = C^+W^+(r,\kappa) , \tag{104a-c}$$

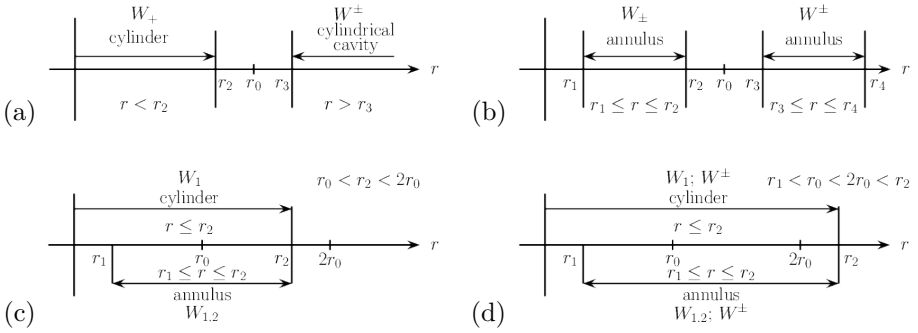

Figure 3: In the case of AVE waves in a cylinder (cylindrical cavity) not containing th critical layer (a) the inner (outer) solution is sufficient; likewise in the case (b of an annulus inside (outside) the critical layer. If the critical layer lies inside (c) a cylinder (cylindrical annulus) with (outer) radius less than twice the critical layer radius, the middle solution is sufficient; if not, the outer solution is also needed, that is for a cylinder (annulus) with (outer) radius larger than twice the critical radius. In all cylindrical cases, the solutions W_+ and W_2 that are singular on axis must be excluded.

	Case	Radius	Solution	Bounded	
				Oscillatory	Monotonic
I	cylindrical cavity	$r_0 < r_3 \le r < \infty$	$C^+W^+(r)$	-	$\kappa^2 < 0$
			$C^+W^+(r) + C^-W^-(r)$	$\kappa^2 > 1$	-
			$C^+W^+(r) + C^-W^-(r)$	-	$0 < \kappa^2 < 1$
II	vortical annulus	$r_0 < r_3 \le r \le r_4 < \infty$	$C^+W^+(r) + C^-W^-(r)$	$\kappa^2 > 1$	$\kappa^2 < 1$
III	acoustic annulus	$0 < r_1 \le r \le r_2 < r_0$	$C_+W_+(r) + C_-W_-(r)$	$\kappa^2 > 0$	$\kappa^2 < 0$
IV	cylinder	$0 \le r \le r_4 < r_0$	$C_+W_+(r)$	$\kappa^2 > 0$	$\kappa^2 < 0$
V	cylindrical annulus	$0 < r_1 \le r \le r_2$ $r_1 < r_0 < r_2$	$C_1W_1(r) + C_2W_2(r)$	$\kappa^2 > 0$	$\kappa^2 < 0$
VI	cylinder	$0 \le r \le r_2$ $r_0 < r_2 < 2r_0$	$C_1W_1(r)$	$\kappa^2 > 0$	$\kappa^2 < 0$

Note: there is no case of unbounded oscillation.

Table 1: Exact solutions of the acoustic-vortical-entropy wave equation indicating the six cases of the stability of the mean flow in the four configurations in the Figure 3.

with the arbitrary constant C^+ determined by one boundary condition at $r = r_3$.

The case II of an annulus outside the critical radius (105a) corresponds to a linear combination of vortical modes (105b),

$$r_0 < r_3 \leq r \leq r_4 < \infty \; : \quad \tilde{v}_r(r,\omega) = C^+ W^+(r,\kappa) + C^- W^-(r,\kappa)\,, \tag{105a, b}$$

with the arbitrary constants $C^\pm$ determined by two boundary conditions at $r = r_3, r_4$. The case III of an annulus inside the critical radius (106a) corresponds to a linear combination of acoustic modes (106b),

$$0 < r_1 \leq r \leq r_2 < r_0 \; : \quad \tilde{v}_r(r,\omega) = C_+ W_+(r,\kappa) + C_- W_-(r,\kappa)\,, \tag{106a, b}$$

with the arbitrary constants $C_\pm$ determined by two boundary conditions at $r = r_1, r_2$. The case IV of a cylinder inside the critical radius (107a) excludes the acoustic mode (59a) with a logarithmic singularity, and involves (107b) only the regular acoustic mode (54b),

$$0 \leq r \leq r_2 < r_0 \; : \quad \tilde{v}_r(r,\omega) = D \sum_{n=0}^{\infty} a_n^+(\kappa)(r/r_0)^{2n+1}\,, \tag{107a, b}$$

where the coefficients (53b) depend on the radial wavenumber. In the case V of a cylindrical annulus containing the critical layer (108a), the middle solution (94b) holds (108c),

$$0 < r_1 \leq r \leq r_2\,, \quad r_1 < r_0 < r_2 < 2r_0 \; : \quad \tilde{v}_r(r,\omega) = C_1 W_1(r,\kappa) + C_2 W_2(r,\kappa)\,, \tag{108a - c}$$

provided that the outer radius is smaller than twice the critical radius (108b). In the case VI of a cylinder (109a), the solution W_2 singular on the axis is excluded (109c),

$$0 \leq r \leq r_2\,, \quad r_0 < r_2 < 2r_0 \; : \quad \tilde{v}_r(r,\omega) = C_1 W_1(r,\kappa)\,. \tag{109a - c}$$

In both cases V and VI, if the outer radius equals or exceeds twice the critical radius, matching to the outer solution is needed to cover the whole annular flow region. Proceeding with case VI and the simplest boundary condition of a rigid wall at $r = a$ with zero radial velocity (110a),

$$\tilde{v}_r(a,\omega) = 0 \; : \quad F(1+\nu/2, 1+\nu/2; 2; a^2/(r_0^2+a^2)) = 0\,, \tag{110a, b}$$

leads to (110b). The Gaussian hypergeometric function in (110b) can be calculated most efficiently summing the series (111a) with the recurrence formula for the successive terms (111c),

$$G(\xi;\nu) \equiv F(1+\nu/2, 1+\nu/2; 2; \xi) = 1 + \sum_{n=1}^{\infty} f_n(\xi)\,, \tag{111a}$$

$$f_0(\xi) = 1\,, \quad f_{n+1}(\xi) = f_n(\xi)\frac{(n+1+\nu/2)^2}{(n+1)(n+2)}\xi\,. \tag{111b, c}$$

The eigenvalues for the radial wavenumber are the roots of (112),

$$0 = G\left(\frac{1}{1+(r_0/a)^2}; \sqrt{1-\kappa^2}\right) = G_0 \prod_{l=1}^{\infty}(\kappa - \kappa_l)\,, \tag{112}$$

where G_0 is a constant. To each eigenvalue corresponds (93a;111a) an eigenfunction,

$$\bar{v}_l(r/r_0) = (1 + r^2/r_0^2)^{-1-\nu/2} G\left(\frac{1}{1+(r_0/r)^2}; \sqrt{1-\kappa^2}\right)\,. \tag{113}$$

The eigenvalues κ_l for the radial wavenumber specify the eigenfrequency $\bar{\omega}_l$ by (40b) with the adiabatic exponent $\gamma = 1.4$ for a diatomic perfect gas.

5.3 Eigenvalues for the wavenumber and frequency and eigenfunctions for six wave variables

The AVE waves are considered inside a cylinder with radius (114a) for the fours cases (114b),

$$0 \leq r \leq a \; : \quad a/r_0 = 0.4, 0.8, 1.2, 1.6 \,, \tag{114a, b}$$

of which the first (last) two do not (do) contain the critical layer. For each cylinder the roots of (110b) specify the first six eigenvalues κ_l of the radial wavenumber ordered by non-decreasing modulus in the Table 2; the corresponding dimensionless natural frequencies $\bar{\omega}_l$ follow from (40b) and appear in the Table 3. To each pair of dimensionless eigenvalues $(\kappa_l, \bar{\omega}_l)$ correspond six dimensionless eigenfunctions for distinct wave variables, namely the dimensionless: (i) radial (107b) velocity (113) with magnitude unity at the origin,

$$D_l \equiv G\left(1; \sqrt{1-\kappa_l^2}\right) \; : \quad \bar{v}_l(r/r_0) = \frac{\tilde{v}_r(r,\omega)}{D_l} \,, \tag{115a, b}$$

that is plotted in the Figure 4; (ii) azimuthal (35a) velocity (116),

$$\bar{w}_l(r/r_0) \equiv \frac{c_{00}}{\Omega r_0} \frac{\tilde{v}_\varphi(r,\omega)}{D_l} = -\mathrm{i} \frac{2}{\bar{\omega}_l} \bar{v}_l(r/r_0) \,, \tag{116}$$

that is plotted in the Figure 5; (iii) the mass (35b) density (117),

$$\bar{\rho}_l(r/r_0) \equiv \frac{c_{00}}{D_l} \frac{\tilde{\rho}}{\rho_0} = -\frac{\mathrm{i}}{\bar{\omega}_l} [\bar{v}_l' + (r_0/r)\bar{v}_l] \,, \tag{117}$$

that is plotted in the Figure 6; (iv) the (35d) entropy (118),

$$\bar{s}_l(r/r_0) \equiv \frac{c_{00}}{D_l} \frac{\tilde{s}(r,\omega)}{C_V} = -\frac{2\mathrm{i}}{\bar{\omega}_l} \frac{1}{r/r_0 + r_0/r} \bar{v}_l \,, \tag{118}$$

that is plotted in the Figure 7; (v) the (35e) pressure (119),

$$\bar{p}_l(r/r_0) \equiv \frac{\tilde{p}(r,\omega)}{\rho_0 c_{00} D_l} = -\frac{\mathrm{i}}{\bar{\omega}_l} \left\{ [(1+2/\gamma)\, r/r_0 + r_0/r]\, \bar{v}_l + \left(1 + r^2/r_0^2\right) \bar{v}_l' \right\} \,, \tag{119}$$

that is plotted in the Figure 8.

The temperature perturbation (35c) follows (121) from those of the density (117) and pressure (119),

$$\begin{aligned} \bar{T}_l(r/r_0) \quad &\equiv \quad \frac{c_{00}}{D_l} \frac{\tilde{T}(r,\omega)}{T_0} = \frac{c_{00}}{\rho_0 D_l} \left[\gamma \frac{\tilde{p}(r,\omega)}{[c_0(r)]^2} - \tilde{\rho}(r,\omega) \right] = \\ &= \quad \frac{\gamma c_{00}^2}{[c_0(r)]^2} \bar{p}_l(r/r_0) - \bar{\rho}_l(r/r_0) = \frac{r_0^2}{2r^2} [M(r)]^2 \bar{p}_l(r/r_0) - \bar{\rho}_l(r/r_0) \,, \end{aligned} \tag{120}$$

that is plotted in the Figure 9. It involves the isothermal swirl Mach number,

$$\gamma \frac{c_{00}^2}{[c_0(r)]^2} = \frac{\gamma^2 \Omega^2 r_0^2}{2[c_0(r)]^2} = \frac{r_0^2}{2r^2} \frac{\gamma^2 \Omega^2 r^2}{[c_0(r)]^2} = \frac{r_0^2}{2r^2} \frac{\Omega^2 r^2}{R T_0} = \frac{r_0^2}{2r^2} [M(r)]^2 \,, \tag{121}$$

where were used (33a,b). In (117) and (119) appear the derivative with regard to its argument (122) of the radial velocity (115),

$$\begin{aligned} \bar{v}_r'(r/r_0) \equiv \frac{\mathrm{d}[\bar{v}_r(r(r_0)]}{\mathrm{d}(r/r_0)} \quad &= \quad -\frac{2+\nu}{D_l} \frac{r}{r_0} \left(1 + r^2/r_0^2\right)^{-2-\nu/2} F\left(1+\nu/2, 1+\nu/2; 2; \xi\right) \\ &+ \quad \frac{(1+\nu/2)^2}{D_l} \frac{r_0^3 r}{(r_0^2 + r^2)^2} F\left(2+\nu/2, 2+\nu/2; 3; \xi\right) \,, \end{aligned} \tag{122}$$

where was used (123a) the derivative (123b) of the Gaussian hypergeometric function in (111a),

$$\frac{\mathrm{d}\xi}{\mathrm{d}(r/r_0)} = \frac{2r_0^3 r}{(r_0^2+r^2)^2}\,, \tag{123a}$$

$$\frac{\mathrm{d}}{\mathrm{d}\xi}\left[F\left(1+\nu/2,1+\nu/2;2;\xi\right)\right] = \frac{(1+\nu/2)^2}{2}F\left(2+\nu/2,2+\nu/2;3;\xi\right). \tag{123b}$$

The Gaussian hypergeometric series in (123b) is calculated as (111a–c) replacing ν by $1+\nu$. The fundamental and first five harmonics are plotted in the Figures 4 to 9 respectively for the dimensionless radial (115) and azimuthal (116) velocity, mass density (117), entropy (118), pressure (119) and temperature (121) perturbations, as basis for the following discussion (Section 7). The radius of the cylindrical duct is taken as the largest $a/r_0 = 1.6$ of the values in (114b) to show the variation of the AVE wave variables across the critical layer.

6 Waveforms for the fundamental and stable and unstable harmonics

The Figures 4 to 9 concern AVE wave modes in a cylindrical duct with rigid wall at a radius $a = 1.6r_0$ that is 60% larger than the radius of the critical layer, thus containing in its interior the radius of isothermal swirl Mach number unity, with subsonic (supersonic) swirl inside (outside). Note that the mean flow is incompressible so there is no restriction on Mach number. The first six modes are considered with dimensionless frequency (40c) indicated in the Table 3, and the corresponding dimensionless radial wavenumbers (40b) on the Table 2. The modulus and phase of the six corresponding eigenfunctions are plotted versus radial distance in the Figure 4 for the radial velocity (115b), in the Figure 5 for the azimuthal velocity (116), in the Figure 6 for the mass density (117), in the Figure 7 for the entropy (118), in the Figure 8 for the pressure (119) and in the Figure 9 for the temperature (121); for all six wave variables are considered as dimensionless perturbation spectra using the amplitude D_l of the radial velocity perturbation spectrum at the axis. For this reason, all waveforms or eigenfunctions start with the value unity on the axis in the Figure 4.

The dimensionless radial velocity perturbation spectra in the Figure 4 all start with the value unity on axis due to the normalization and all finish with zero at the rigid wall at $r = 1.6r_0 = a$. The fundamental mode $\bar{v}_1$ has no other zero, and decays smoothly from the axis to the wall. As typical of eigenvalue problems, the harmonics $\bar{v}_n$ of order $n = 2, 3, 4$ have $n-1$ zeros of the amplitude (Figure 4 top) between the axis and the wall, corresponding to phase jumps of π (Figure 4 bottom). The fifth and sixth harmonics $n = 5, 6$ have complex radial wavenumbers in the Table 2, leading to radially decaying or divergent modes; the divergent modes signal instabilities of the mean as can be seen from the increasing amplitudes of $\bar{v}_5^+$ and $\bar{v}_6^+$ (Figure 4 top). The dimensionless azimuthal velocity perturbation spectrum (Figure 5) also vanishes at the rigid wall for the fundamental $\bar{w}_1$ and next three harmonics $\bar{w}_2$, $\bar{w}_3$, $\bar{w}_4$ (Figure 5 top), again with phase jumps of π at the zeros of the amplitude or nodes (Figure 5 bottom). The fifth and sixth harmonics $\bar{w}_5^+$, $\bar{w}_6^+$ are unstable modes both for the radial (Figure 4 top) and azimuthal (Figure 5 top) velocity perturbations spectra. The amplitude of the dimensionless azimuthal velocity perturbation spectrum on axis (Figure 5 top) decreases from the fundamental to the higher harmonics.

The perturbation spectrum of the mass density (Figure 6) leads to eigenfunctions that are quite different from those of the radial (Figure 4) and azimuthal (Figure 5) velocity perturbation spectra. The mass density perturbation spectra do not vanish at the rigid wall (Figure 6 top) although their magnitude decreases from the fundamental $\bar{\rho}_1$ to the next three stable harmonics $\bar{\rho}_2$, $\bar{\rho}_3$, $\bar{\rho}_4$. The fundamental $\bar{\rho}_1$ almost vanishes at $r = 0.48r_0$ leading to rapid phase change of π (Figure 6 bottom). Whereas the fundamental $\bar{\rho}_1$ has one dip, the next three $n = 2, 3, 4$ harmonics $\bar{\rho}_n$ have n dips, and the fifth and sixth harmonics $\bar{\rho}_5^+$, $\bar{\rho}_6^+$ are unstable as before. The dimensionless entropy perturbation spectrum (Figure 7) vanishes on axis for all harmonics , including the unstable ones $\bar{s}_5^+$, $\bar{s}_6^+$, and vanishes also at the rigid wall for the fundamental $\bar{s}_1$ and the first three stable harmonics $\bar{s}_2$, $\bar{s}_3$, $\bar{s}_4$. The fundamental $\bar{s}_1$ has no zeros and exhibits a single peak at $r = 0.5r_0$ far from the critical layer. The first three harmonics $\bar{s}_n$ with $n = 2, 3, 4$ have n peaks and $n-1$ nodes.

The peaks are lower when: (i) passing from the fundamental $n = 1$ to the harmonics $n = 2, 3, 4$; (ii) for a given harmonic n, the successive n peaks become lower farther from the axis.

The dimensionless pressure perturbation spectra (Figure 8) are broadly similar to those of the mass density (Figure 6), with similar features, such as a non-zero pressure at the rigid wall with amplitude decreasing from the fundamental $\bar{p}_1$ to the first three stable harmonics $\bar{p}_2$, $\bar{p}_3$, $\bar{p}_4$. The fifth and sixth harmonics $\bar{p}_5^+$, $\bar{p}_6^+$ remain unstable. The fundamental $\bar{p}_1$ has one dip of the amplitude (Figure 8 top) broader than for the mass density (Figure 6 top) and approximately at the same location $r = 0.48 r_0$. The next three stable harmonics $\bar{p}_n$ with $n = 2, 3, 4$ have n dips and n peaks (Figure 8 top) with phase jumps (Figure 8 bottom) indicating that the dips are actually zeros or nodes. The dimensionless temperature perturbation spectra (Figure 9) have eigenfunctions broadly similar to the entropy (Figure 7), with: (i) zero on axis for all modes, stable $\bar{T}_1$, $\bar{T}_2$, $\bar{T}_3$, $\bar{T}_4$ or unstable $\bar{T}_5^+$, $\bar{T}_6^+$; (ii) the stable modes are also zero at the wall; (iii) the fundamental mode $\bar{T}_1$ has a single maximum between the axis and the wall; (iv) the stable harmonics $n = 2, 3, 4$ have n maxima and $n - 1$ zeros.

Thus besides the unstable diverging spectra, there are three kinds of stable spectra for the fundamental mode $n = 1$ (first three harmonics $n = 2, 3, 4$): (i) monotonic (oscillatory) decay for the dimensionless radial (Figure 4) and azimuthal (Figure 5) velocity perturbation spectra, that are non-zero on axis and zero at the wall; (ii) non-zero at the wall for the dimensionless mass density (Figure 6) and pressure (Figure 8) perturbation spectra with a single dip (n dips and $n - 1$ maxima); (iii) zero on axis and at the wall for the dimensionless entropy (Figure 7) and temperature (Figure 9) perturbation spectra with a single maximum (n maxima and $n - 1$ zeros).

7 Discussion

The present paper may be the first to combine the interactions of the three types of waves in a fluid not subject to external force fields, hence the designation acoustic-vortical-entropy (AVE) waves. A deliberate choice was made of one of the simplest baseline flows that could support AVE waves, namely an incompressible non-isentropic uniform flow with rigid body swirl, leading to a mean flow pressure and sound speed varying radially due to the centrifugal force. The linear non-dissipative perturbation of this mean flow leads in the axisymmetric case to the AVE wave equations (27;28a-c) first obtained here. The exact solution is obtained in terms of Gaussian hypergeometric functions in the case of zero axial wavenumber, when there is only temporal and radial dependences. The six wave variables in this case are the frequency spectra of the perturbations of the (i) radial and (ii) azimuthal velocity, (iii) mass density, (iv) entropy, (v) pressure and (vi) temperature.

An important feature of the problem is the existence of a critical layer where the swirl velocity equals the isothermal sound speed. It is shown that this condition of isothermal swirl Mach number unity corresponds to a finite wave field, and thus is a singularity of the AVE wave equation but not a singularity of the wave field. The linear non-dissipative non-isentropic compressible vortical perturbations of the non-isentropic uniform flow with rigid swirl may be interpreted alternatively as (i) acoustic-vortical entropy (AVE) waves or (ii) stability or instability modes of the mean flow. This dual interpretation is demonstrated for a cylindrical duct with rigid wall at the radius $a = 1.6 r_0$, that is 60% larger than the critical layer, for: (a) the eigenvalues for the wavenumber (Table 2) and frequency (Table 3); (b) the eigenfunctions for the radial (Figure 4) and azimuthal (Figure 5) velocity, mass density (Figure 6), entropy (Figure 7), pressure (Figure 8) and temperature (Figure 9). These confirm that the wave field is finite at the critical layer in this as well as in all other cases; in this particular case, the fundamental and first three harmonics are stable and the fifth and sixth harmonics are unstable. The general theory applies to all cases of cylindrical or annular ducts or cylindrical cavities containing or not the critical layer.

Acknowledgements

This work was supported by FCT (Foundation for Science and Technology) through IDMEC (Institute of Mechanical Engineering), under LAETA Pest-OE/EME/LA0022.

$0 \le r \le r_1$	$r_1 = 0.4r_0$	$r_1 = 0.8r_0$	$r_1 = 1.2r_0$	$r_1 = 1.6r_0$
κ_1	9.874	5.322	3.895	3.217
κ_2	18.015	9.626	6.974	5.700
κ_3	26.103	13.920	10.061	8.203
κ_4	34.175	18.212	13.150	10.712
κ_5	42.240	22.502	16.241	13.027±i14.338
κ_6	50.302	26.791	18.195±i27.868	15.588±i7.640

Table 2: First six eigenvalues of the radial wavenumber for acoustic-vortical-entropy waves in a cylinder $0 \le r \le r_1$ with rigid wall with radius r_1 a fraction of the critical radius.

$0 \le r \le r_1$	$r_1 = 0.4r_0$	$r_1 = 0.8r_0$	$r_1 = 1.2r_0$	$r_1 = 1.6r_0$
$\bar{\omega}_1$	10.110	5.748	4.460	3.881
$\bar{\omega}_2$	18.145	9.868	7.304	6.100
$\bar{\omega}_3$	26.193	14.089	10.293	8.485
$\bar{\omega}_4$	34.244	18.341	13.329	10.930
$\bar{\omega}_5$	42.296	22.606	16.386	13.109±i14.248
$\bar{\omega}_6$	50.349	26.879	18.234±i27.809	15.710±i7.581

Table 3: As the Table 2 for the corresponding values of the dimensionless frequency.

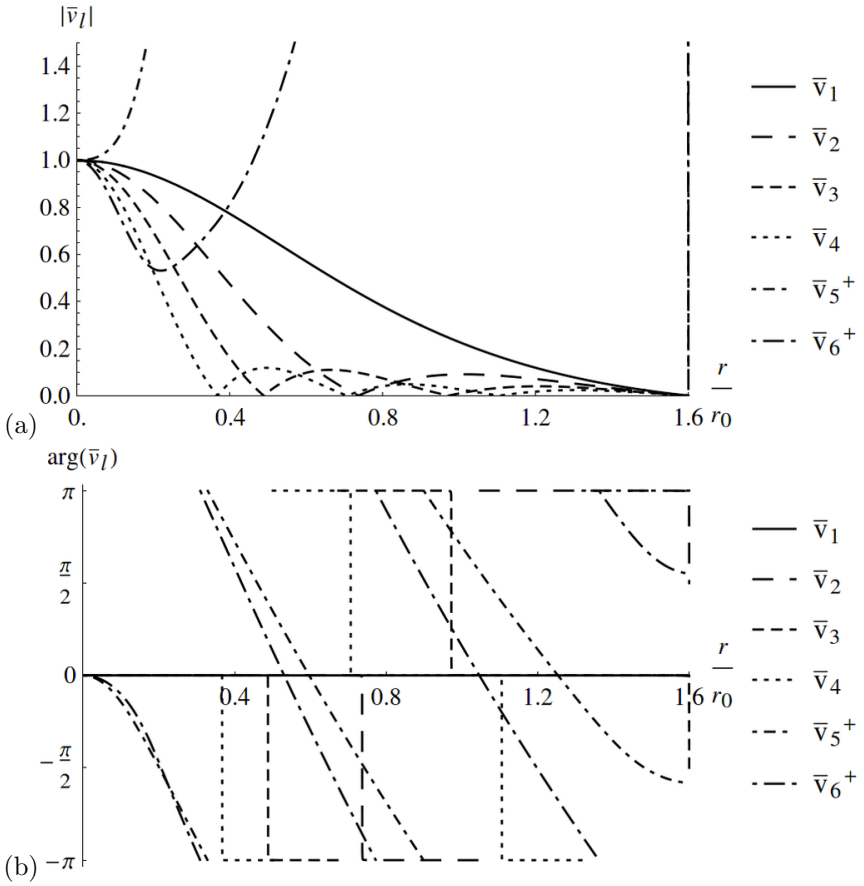

Figure 4: Modulus (top) and phase (bottom) versus radial distance normalized to the critical radius, for dimensionless radial velocity perturbation spectrum, of the first six modes of acoustic-vortical-entropy waves in a rigid cylinder with radius equal to 1.6 of the critical radius.

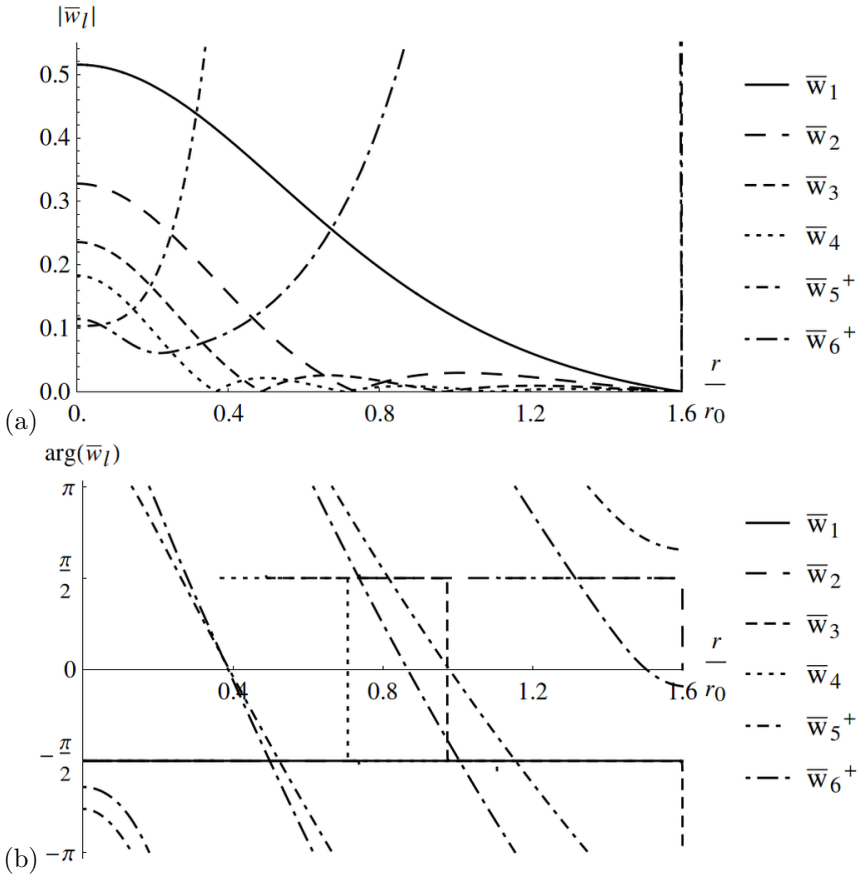

Figure 5: As of Figure 4 for the dimensionless azimuthal velocity perturbation spectrum.

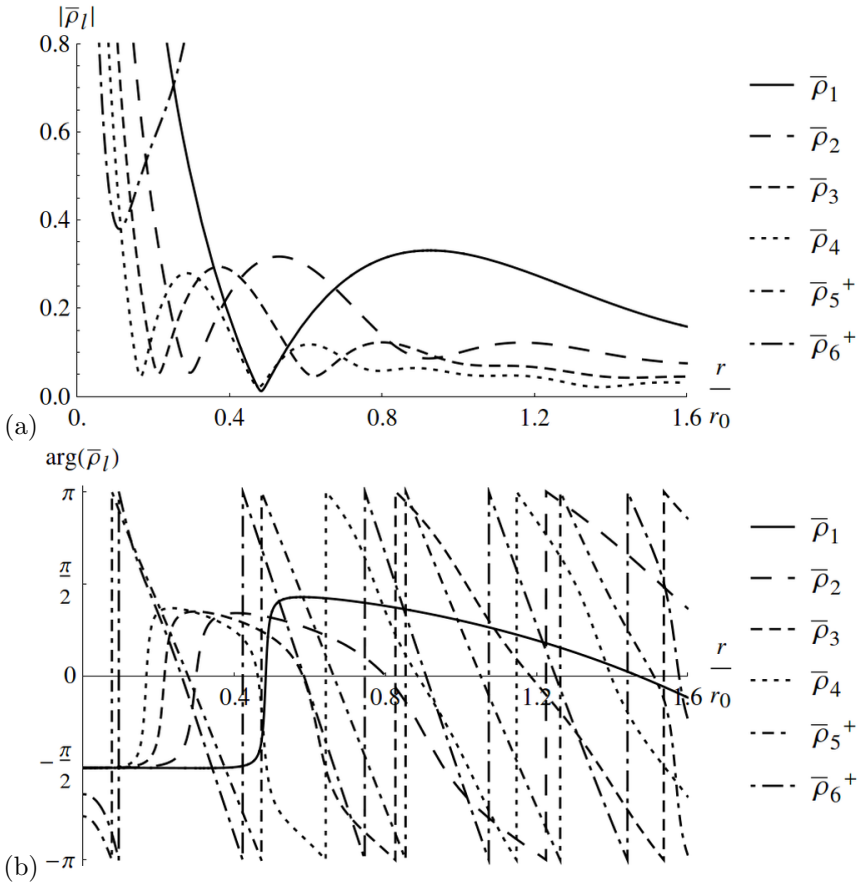

Figure 6: As of Figure 4 for the dimensionless mass density perturbation spectrum.

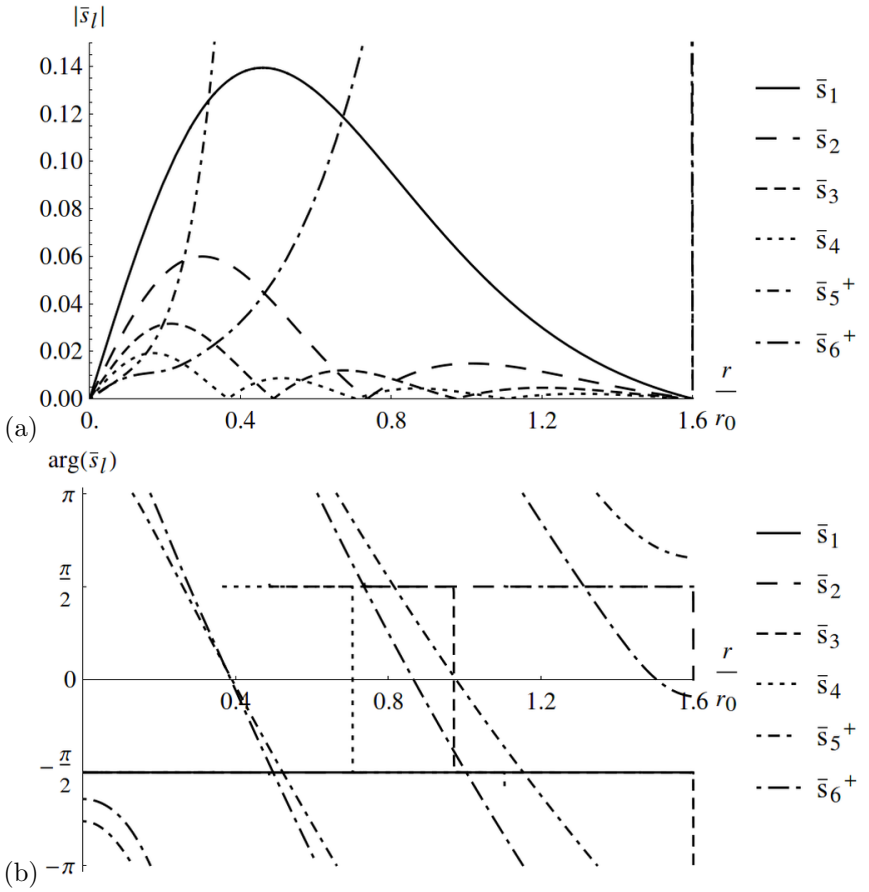

Figure 7: As of Figure 4 for the dimensionless entropy perturbation spectrum.

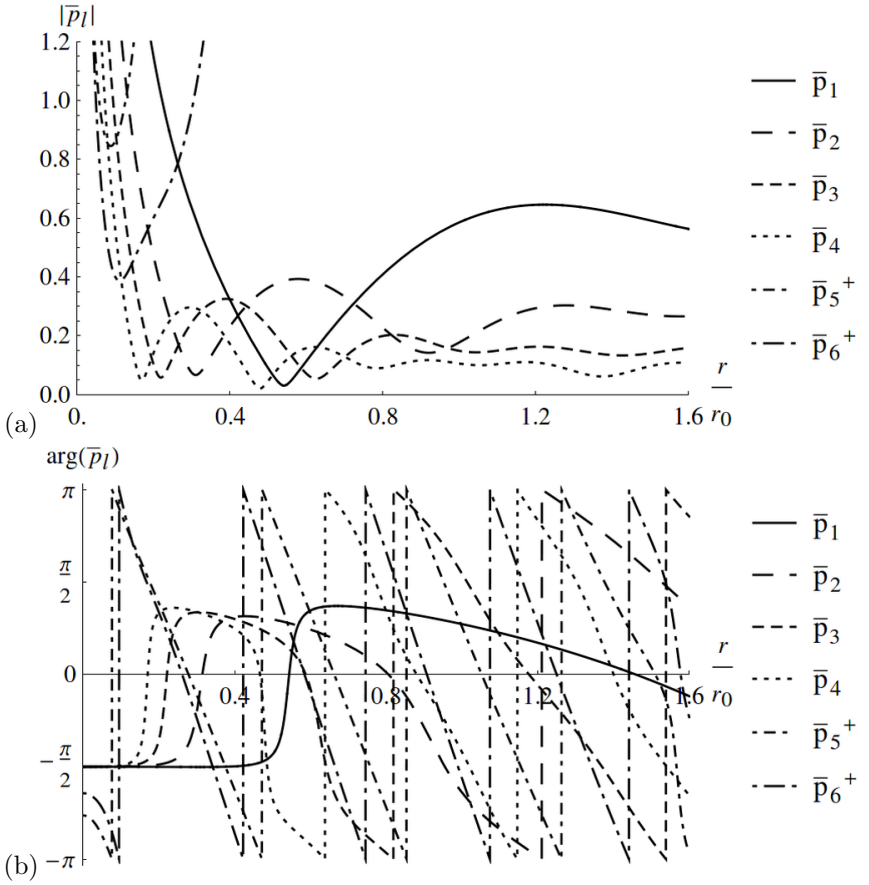

Figure 8: As of Figure 4 for the dimensionless pressure perturbation spectrum.

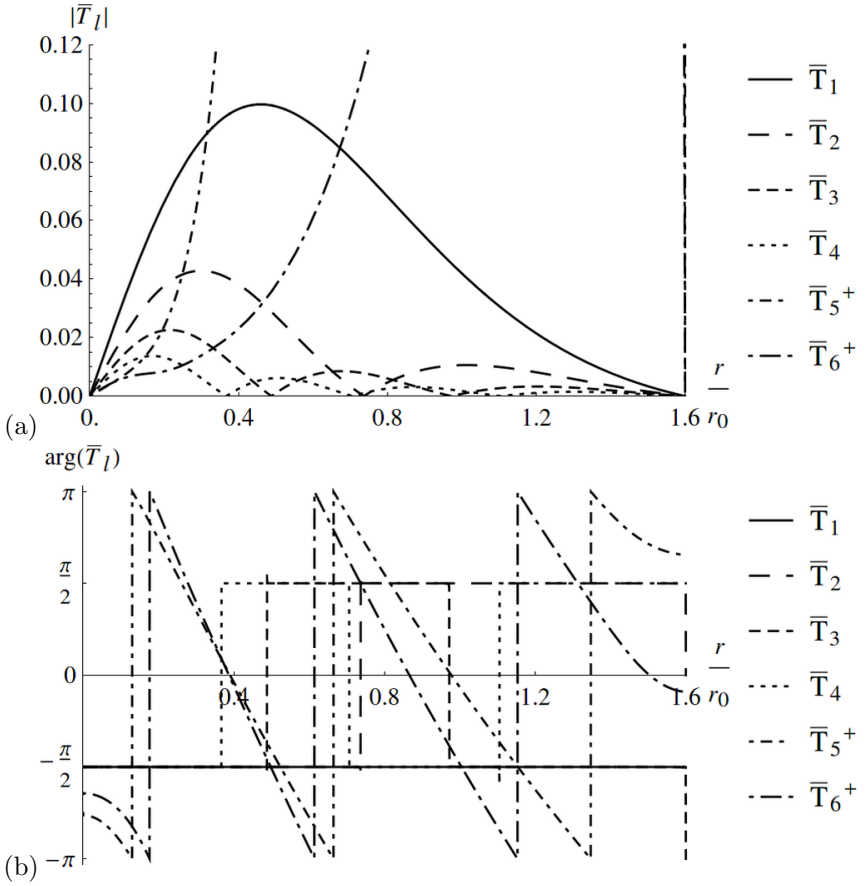

Figure 9: As of Figure 4 for the dimensionless temperature perturbation spectrum.

References

References

[1] L. S. G. Kovasznay, Turbulence in supersonic flow, J Aero Sci 20 (10) (1953) 657–674.

[2] L. D. Landau, E. M. Lifshitz, Fluid Mechanics, Vol. 6 of Course of Theoretical Physics, Pergamon Press, 1959, ISBN:9780080091044.

[3] A. D. Pierce, Acoustics: An Introduction to Its Physical Principles and Applications, McGraw-Hill, 1981, ISBN:9780883186121.

[4] L. M. B. C. Campos, On the generation and radiation of magneto-acoustic waves, J Fluid Mech 81 (3) (1977) 529–549, doi:10.1017/S0022112077002213.

[5] L. M. B. C. Campos, On magnetoacoustic-gravity-inertial (MAGI) waves I. generation, propagation, dissipation and radiation, Mon Not R Astron Soc 410 (2) (2011) 717–734, doi:10.1111/j.1365-2966.2010.17553.x.

[6] J. W. S. Rayleigh, The Theory of Sound, 2^{nd} Edition, Vol. 2 Vols. of Dover Books on Physics, Dover Publications, 1945 (reprint), 1877, ISBN:9780486602929.

[7] P. M. Morse, K. U. Ingard, Theoretical Acoustics, McGraw-Hill, 1968, ISBN:0691084254.

[8] M. E. Goldstein, Aeroacoustics, McGraw-Hill, 1976, ISBN:9780070236851.

[9] J. Lighthill, Waves in Fluids, Cambridge Mathematical Library, Cambridge U.P., 1978, ISBN:9780521010450.

[10] A. P. Dowling, J. E. Ffowcs-Williams, Sound and Sources of Sound, Ellis Horwood, 1983, ISBN:9780853125273.

[11] T. D. Rossing (Ed.), Handbook of Acoustics, Springer handbooks, Springer, 2007, ISBN:9780387336336.

[12] M. J. Crocker (Ed.), Handbook of Noise and Vibration Control, Wiley, 2007, ISBN:9780471395997.

[13] H. Lamb, Hydrodynamics, 5^{th} Edition, Cambridge Mathematical Library, Cambridge U.P., 1932, ISBN:0521055156.

[14] L. M. Milne-Thomson, Theoretical Hydrodynamics, Dover, 1968, ISBN:0486689700.

[15] J. Lighthill, An Informal Introduction to Theoretical Fluid Mechanics, Institute of Mathematics & its Applications Monograph Series, Cambridge U.P., 1988, ISBN:9780198536307.

[16] M. S. Howe, Hydrodynamics and Sound, Cambridge U.P., 2006, ISBN:9780521868624.

[17] L. M. B. C. Campos, Complex Analysis with Applications to Flows and Fields, Vol. 1 of Mathematics and Physics in Science and Engineering, CRC Press, 2010, ISBN:9781420071184.

[18] M. S. Howe, Contributions to the theory of aerodynamic sound, with application to excess jet noise and the theory of the flute, J Fluid Mech 71 (5) (1975) 625–673, doi:10.1017/S0022112075002777.

[19] L. M. B. C. Campos, On the emission of sound by an ionized inhomogeneity, P Roy Soc Lond A Mat 359 (1696) (1978) 65–91, doi:10.1098/rspa.1978.0032.

[20] L. M. B. C. Campos, F. J. P. Lau, On sound generation by moving surfaces and convected sources in a flow, Int J Aeroacoust 11 (1) (2012) 103–136, doi:10.1260/1475-472X.11.1.103.

[21] L. M. B. C. Campos, On linear and non-linear wave equations for the acoustics of high-speed potential flows, J Sound Vib 110 (1) (1986) 41–57, doi:10.1016/S0022-460X(86)80072-4.

[22] L. M. B. C. Campos, On waves in gases. part I: Acoustics of jets, turbulence, and ducts, Rev Mod Phys 58 (1) (1986) 117–182, doi:10.1103/RevModPhys.58.117.

[23] L. M. B. C. Campos, On the generalizations of the doppler factor, local frequency, wave invariant and group velocity, Wave Motion 10 (3) (1988) 193–207, doi:10.1016/0165-2125(88)90018-2.

[24] W. Haurwitz, Zur theorie der wellenbewegungen in luft und wasser ("on the theory of wave perturbations in a flow in air and water"), Veröffentlichungen des Geophysikalischen Instituts der Karl-Marx-Universität Leipzig 6 (1) (1931) 334–364.

[25] D. Küchemann, Störungsbewegungen in einer gasströmung mit grenzschicht, Z Angew Math Mech 18 (4) (1938) 207–222, doi:10.1002/zamm.19380180402.

[26] D. C. Pridmore-Brown, Sound propagation in a fluid flowing through an attenuating duct, J Fluid Mech 4 (4) (1958) 393–406, doi:10.1017/S0022112058000537.

[27] W. Möhring, E. Müller, F. Obermeier, Problems in flow acoustics, Rev Mod Phys 55 (3) (1983) 707–724, doi:10.1103/RevModPhys.55.707.

[28] L. M. B. C. Campos, On 36 forms of the acoustic wave equation in potential flows and inhomogeneous media, Appl Mech Rev 60 (4) (2007) 149–171, doi:10.1115/1.2750670.

[29] L. M. B. C. Campos, On 24 forms of the acoustic wave equation in vortical flows and dissipative media, Appl Mech Rev 60 (6) (2007) 291–315, doi:10.1115/1.2804329.

[30] M. Goldstein, E. Rice, Effect of shear on duct wall impedance, J Sound Vib 30 (1) (1973) 79–84, doi:10.1016/S0022-460X(73)80051-3.

[31] D. S. Jones, The scattering of sound by a simple shear layer, Phil Trans R Soc Lond A 284 (1323) (1977) 287–328, doi:10.1098/rsta.1977.0011.

[32] D. S. Jones, Acoustics of a splitter plate, IMA J Appl Math 21 (2) (1978) 197–209, doi:10.1093/imamat/21.2.197.

[33] S. P. Koutsoyannis, Characterization of acoustic disturbances in linearly sheared flows, J Sound Vib 68 (2) (1980) 187–202, doi:10.1016/0022-460X(80)90464-2.

[34] S. P. Koutsoyannis, K. Karamcheti, D. C. Galant, Acoustic resonances and sound scattering by a shear layer, AIAA J 18 (12) (1980) 1446–1454, doi:10.2514/3.7736.

[35] J. N. Scott, Propagation of sound waves through a linear shear layer, AIAA J 17 (3) (1979) 237–244, doi:10.2514/3.61107.

[36] L. M. B. C. Campos, J. M. G. S. Oliveira, M. H. Kobayashi, On sound propagation in a linear shear flow, J Sound Vib 219 (5) (1999) 739–770, doi:10.1006/jsvi.1998.1880.

[37] L. M. B. C. Campos, P. G. T. A. Serrão, On the acoustics of an exponential boundary layer, Phil Trans R Soc Lond A 356 (1746) (1998) 2335–2378, doi:10.1098/rsta.1998.0277.

[38] L. M. B. C. Campos, M. H. Kobayashi, On the reflection and transmission of sound in a thick shear layer, J Fluid Mech 424 (2000) 303–326, doi:10.1017/S0022112000002068.

[39] L. M. B. C. Campos, J. M. G. S. Oliveira, On the acoustic modes in a duct containing a parabolic shear flow, J Sound Vib 330 (6) (2011) 1166–1195, doi:10.1016/j.jsv.2010.09.021.

[40] L. M. B. C. Campos, M. H. Kobayashi, On the propagation of sound in a high-speed non-isothermal shear flow, Int J Aeroacoust 8 (3) (2009) 199–230, doi:10.1260/147547208786940035.

[41] L. M. B. C. Campos, M. H. Kobayashi, Sound transmission from a source outside a non-isothermal boundary layer, AIAA J 48 (5) (2010) 878–892, doi:10.2514/1.40674.

[42] L. M. B. C. Campos, M. H. Kobayashi, On an acoustic oscillation energy for shear flows, Int J Aeroacoust 12 (1) (2013) 123–168, doi:10.1260/1475-472X.12.1-2.123.

[43] L. M. B. C. Campos, M. H. Kobayashi, On sound emission by sources in a shear flow, Int J Aeroacoust 12 (7-8) (2013) 719–742, doi:10.1260/1475-472X.12.7-8.719.

[44] V. V. Gobulev, H. M. Atassi, Sound propagation in an annular duct with mean potential swirling flow, J Sound Vib 198 (5) (1996) 601–616, doi:10.1006/jsvi.1996.0591.

[45] V. V. Gobulev, H. M. Atassi, Acoustic-vorticy waves in swirling flows, J Sound Vib 209 (2) (1998) 203–222, doi:10.1006/jsvi.1997.1049.

[46] L. M. B. C. Campos, P. G. T. A. Serrão, On the sound in unbounded and ducted vortex flows, SIAM J Appl Math 65 (4) (2005) 1353–1368, doi:10.1137/S0036139903427076.

[47] C. K. W. Tam, L. Auriault, The wave modes in ducted swirling flows, J Fluid Mech 371 (1) (1998) 1–20, doi:10.1017/S0022112098002043.

[48] M. E. Goldstein, Unsteady vortical and entropic distortions of potential flows round arbitrary obstacles, J Fluid Mech 89 (3) (1978) 433–468, doi:10.1017/S0022112078002682.

[49] C. J. Heaton, N. Peake, Acoustic scattering in a duct with mean swirling flow, J Fluid Mech 540 (2005) 189–220, doi:10.1017/S0022112005005719.

[50] C. J. Heaton, N. Peake, Algebraic and exponential instability of inviscid swirling flow, J Fluid Mech 565 (2006) 279–318, doi:10.1017/S0022112006001698.

[51] L. M. B. C. Campos, P. G. T. A. Serrão, On the continuous and discrete spectrum of acoustic-vortical waves, Int J Aeroacoust 12 (7-8) (2013) 743–782, doi:10.1260/1475-472X.12.7-8.743.

[52] A. Powell, Theory of vortex sound, J Acoust Soc Am 36 (1) (1964) 177–195, doi:10.1121/1.1918931.

[53] M. S. Howe, Theory of vortex sound, Cambridge Texts in Applied Mathematics, Cambridge U.P., 2002, ISBN:9780521012232.

[54] C. C. Lin, The Theory of Hydrodynamic Stability, Cambridge Monographs on Mechanics Applied Mathematics, Cambridge U.P., 1955, aSIN:B0000CJB1L.

[55] S. Chandrasekhar, Hydrodynamic and Hydromagnetic Stability, Oxford U.P., 1961, ISBN:978-0486640716.

[56] D. D. Joseph, Stability of fluid motions. I,II, Vol. 27 & 28 of Springer Tracts in Natural Philosophy, Springer-Verlag, 1976, ISBN:9780471116219.

[57] P. G. Drazin, W. H. Reid, Hydrodynamic Stability, Cambridge monographs on mechanics and applied mathematics, Cambridge U.P., 1981, ISBN:0521227984.

[58] L. M. B. C. Campos, Transcendental Representations with applications to Solids and Fluids, Vol. 2 of Mathematics and Physics in Science and Engineering, CRC Press, 2012, ISBN:9781439834312.

[59] E. L. Ince, Ordinary Differential Equations, Dover, 1956, ISBN:9780486603490.

[60] A. R. Forsyth, A Treatise on Differential Equations, Dover, 1929, ISBN:9780486693149.

[61] E. T. Whittaker, G. N. Watson, A Course of Modern Analysis, Cambridge UP, 1927, ISBN:9781603864541.

[62] C. Carathéodory, Theory of Functions of a Complex Variable, Vol. 1–2, Verlag Birkhauser, 1950, ISBN:9780821828311.

[63] M. J. Lighthill, Notes on the hypergeometric function, lecture notes - private communication (1978).

[64] E. Copson, Theory of Functions of a Complex Variable, Oxford, 1935, ISBN: 9780198531456.

[65] L. M. B. C. Campos, Generalized Calculus with Applications to Matter and Forces, CRC Press, 2014, ISBN: 9781420071153.

[66] A. Erdélyi (Ed.), Higher Transcendental Functions, Vol. 1–3, McGraw-Hill, 1953, ASIN:B005Z5A43I.

[67] M. Abramowitz, I. A. Stegun (Eds.), Handbook of mathematical functions, Vol. 55 of Dover Books on Advanced Mathematics, Dover, 1965, ISBN:9780486612720.

[68] T. Bromwich, T. M. MacRobert, An Introduction to the Theory of Infinite Series, MacMillan, 1926, ISBN:9781164810001.

[69] K. Knopp, Theory and Application of Infinite Series, Dover (reprint 1990, 1921, ISBN:9780486661650.